Angewandte Chemie
Eine Zeitschrift der Gesellschaft Deutscher Chemiker

Supporting Information

69451 Weinheim, Germany

A Versatile Ligand Platform that Supports Lewis Acid Promoted Migratory Insertion**

Amaruka Hazari, Jay A. Labinger, and John E. Bercaw**

anie_201203264_sm_miscellaneous_information.pdf

Supporting Information

Table of Contents

Experimental Section

S1: Materials and Methods

All air- and moisture-sensitive compounds were manipulated using standard vacuum line or Schlenk techniques, or in a glovebox under a nitrogen atmosphere. The solvents for air- and moisture-sensitive reactions were dried with activated alumina by the method of Grubbs.[23] All NMR solvents were purchased from Cambridge Isotope Laboratories Inc. Benzene-d_6 was distilled from sodium benzophenone ketyl or titanocene. Dichloromethane-d_2 and acetonitrile-d_3 were distilled from calcium hydride and run through a small column of activated alumina. Tetrahydrofuran-d_8 was purchased in a sealed ampoule, and dried by passage through activated alumina. Unless noted, other materials were used as received. $Re(CO)_5Br$ was purchased from Strem Chemicals, and monoaza-12-crown-4 was purchased from TCI Chemicals. $[Re(CO)_4(\mu\text{-}Br)]_2$,[24] $CaI_2(THF_4)$,[25] $SrI_2(THF)_5$[25] and $MgX_2(THF)_n$[26, 27] were synthesized according to literature procedures. Elemental analyses were performed by Midwest Microlab, IN. ^1H and ^{13}C NMR spectra were recorded on Varian Mercury 300 MHz, or Varian 500 MHz spectrometers at room temperature, unless indicated otherwise. Chemical shifts are reported with respect to residual internal protio solvent for ^1H and $^{13}C\{^1H\}$ spectra. ^{31}P NMR spectra were referenced to external 85% H_3PO_4. X-ray crystallography was carried out by Dr. Michael W. Day and Lawrence M. Henling using a Bruker KAPPA APEXII X-ray diffractometer.

S2: Synthesis of Complexes 2-6.

$PPh_2CH_2NCH_2(CH_2OCH_2)_3CH_2$ (PNO) (2). Monoaza-12-crown-4 (1 g, 5.74 mmol) and diphenylphosphine (1.07 g, 5.74 mmol) were dissolved in 20 ml of THF. Aqueous formaldehyde (0.512 ml of a 37 % solution, 7.46 mmol) was added and the reaction mixture was heated to 60 °C for 2 h. The mixture was dried over anhydrous magnesium sulfate, filtered, and the filtrate evaporated to a pale yellow oil. The oil was extracted into pentane and evaporated to afford the product as a colorless oil (1.7 g, 80%). ^{1}H NMR (500 MHz, C_6D_6, δ, ppm): 7.57-7.53 (m, 4H), 7.14-7.05 (m, 6H), 3.59 (t, 4H, J = 5 Hz), 3.44-3.39 (m, 8H), 3.32 (d, 4H, J = 5 Hz), 2.93 (t, 4H, J = 5 Hz); ^{13}C NMR (125.7 MHz, C_6D_6, δ, ppm): 139.5 (d, J = 13.8 Hz), 133.6 (d, J = 17.6 Hz), 128.6 (d, J = 6.3 Hz), 71.8, 70.6 (d, J = 8.8 Hz), 61.5 (d, J = 5.0 Hz), 57.0 (d, 7.5 Hz); ^{31}P NMR (121.5 MHz, C_6D_6, δ, ppm): - 26.3. Elemental analysis $C_{21}H_{28}NO_3P$: Calcd: C, 67.54; H, 7.56; N, 3.75. Found: C, 67.77; H, 7.34; N, 3.50.

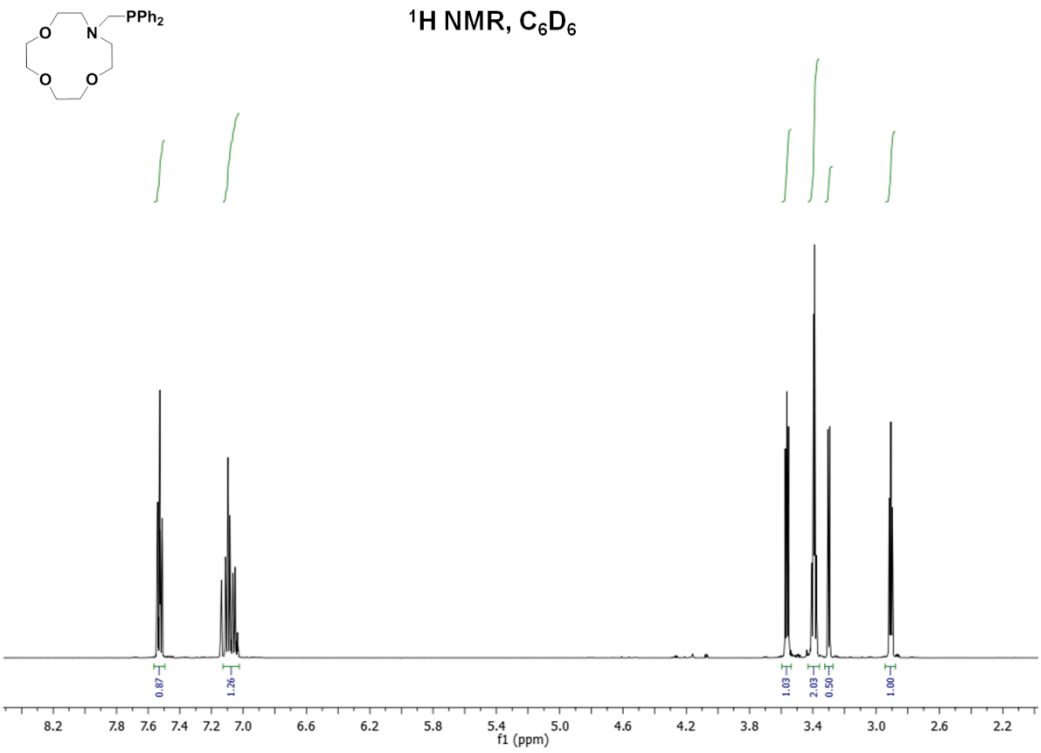

Figure S1. ^{1}H NMR spectrum of **2**.

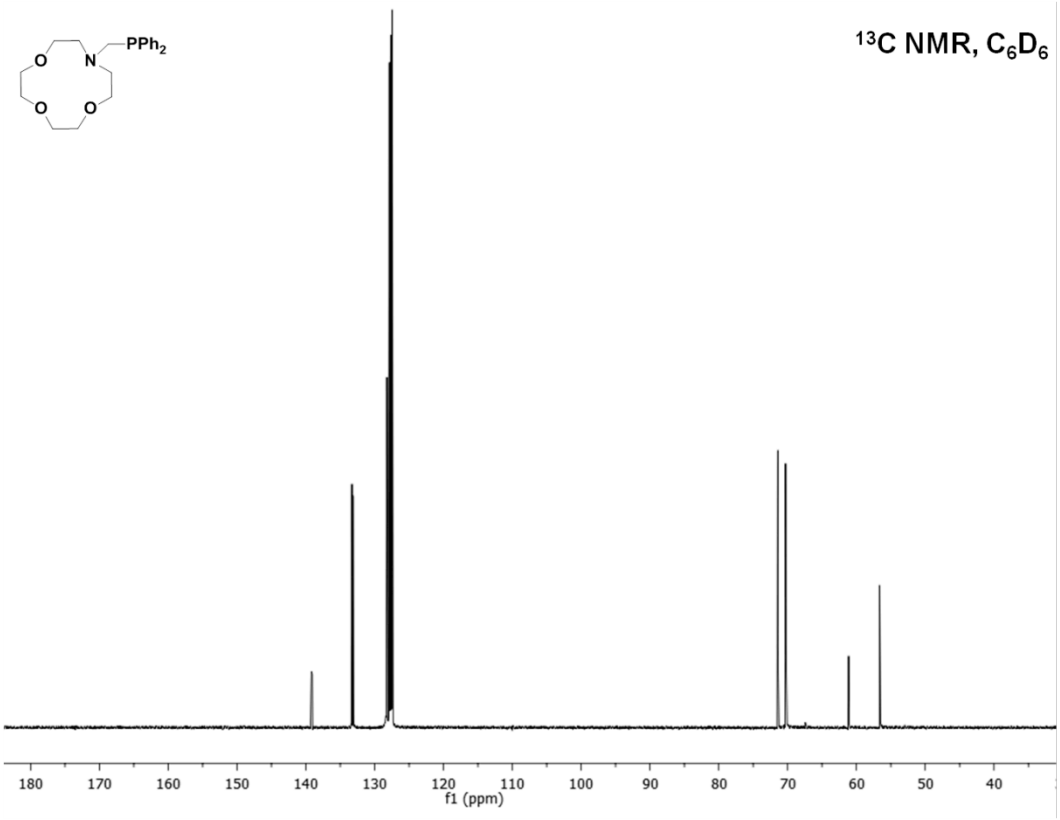

Figure S2. ^{13}C NMR spectrum of **2**.

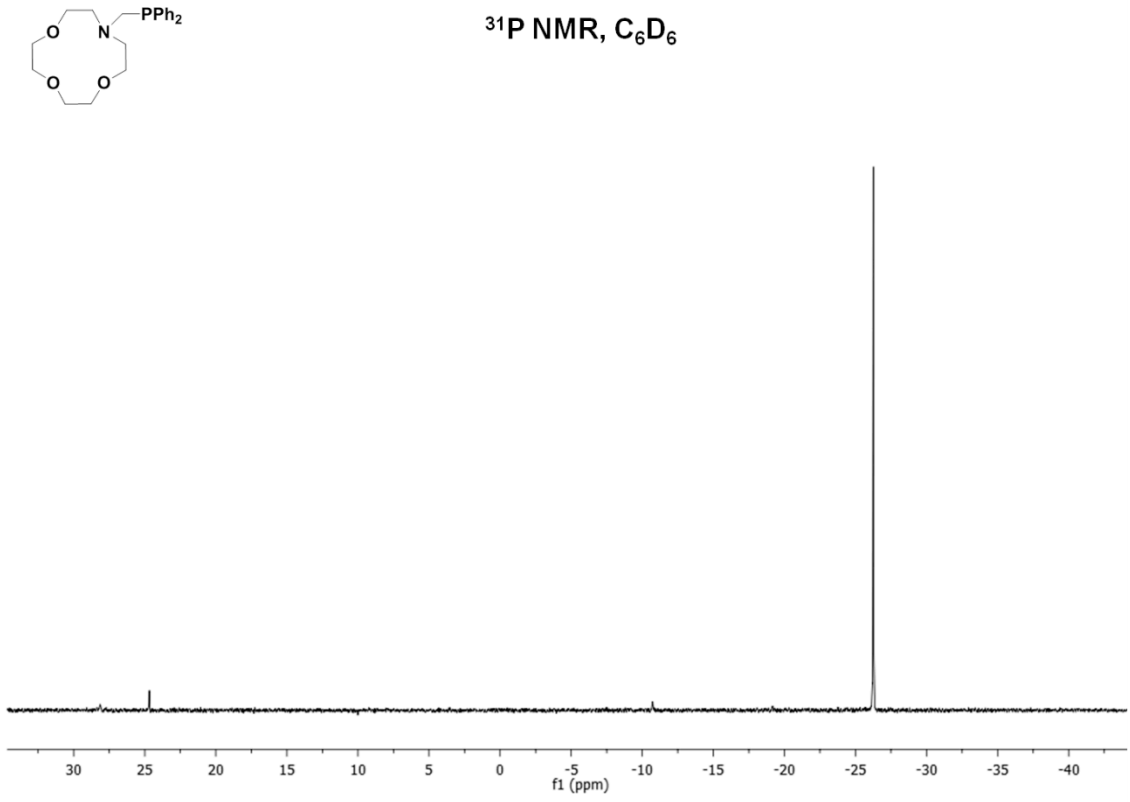

Figure S3. ^{31}P NMR spectrum of **2**.

$Re(CO)_4(PNO)Br$ (3). $[Re(CO)_4(\mu\text{-}Br)]_2$ (1.8 g, 2.38 mmol) was added to a solution of the ligand **2** (1 g, 2.68 mmol) in THF (15 ml). The suspension was stirred for 12 h during which time a pale yellow solution formed. The solvent was evaporated *in vacuo* and the residue extracted with dichloromethane. The dichloromethane solution was evaporated and the product washed with pentane and dried *in vacuo* to afford a white solid (1.6 g, 79%). ^1H NMR (500 MHz, C_6D_6, δ, ppm): 7.70-7.64 (m, 4H), 7.55-7.47 (m, 6H), 4.23 (d, 2H, J = 1.5 Hz), 3.56-3.53 (m, 4H), 3.48-3.43 (m, 8H), 2.60 (t, 4H, J = 5 Hz); ^{13}C NMR (100.54 MHz, CD_2Cl_2, δ, ppm): 185.54 (d, J = 8.8 Hz), 185.09 (d, J = 6.3 Hz), 184.51 (d, J = 54.8 Hz), 133.82 (d, J = 10.1 Hz), 132.66 (d, J = 45.3 Hz), 132.52 (d, J = 5 Hz), 129.2 (d, J = 8.8 Hz), 72.1, 70.5, 69.9, 56.2 (d, J = 37.7 Hz), 55.2 (d, J = 2.5 Hz); ^{31}P NMR (121.5 MHz, C_6D_6, δ, ppm): - 4.0 (s). IR (CH_2Cl_2, cm^{-1}): 2100, 2046, 2007, 1939. Elemental analysis $C_{25}H_{28}BrNO_7PRe$: Calcd: C, 39.95; H, 3.76; N, 1.86. Found: C, 39.62; H, 3.76; N, 1.86.

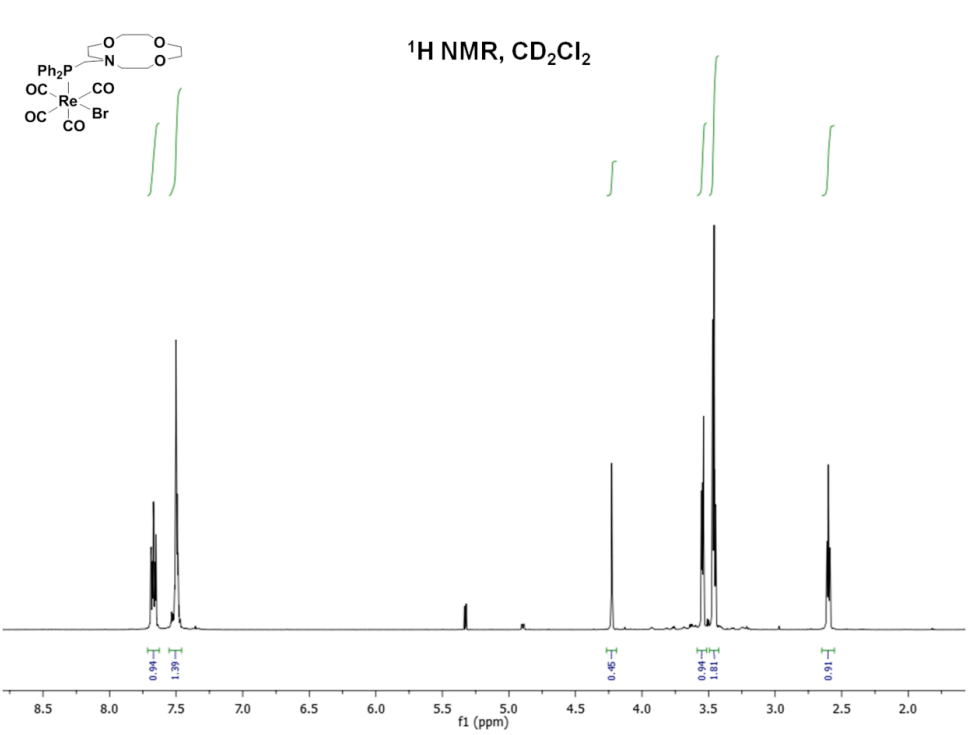

Figure S4. ^{1}H NMR spectrum of **3**.

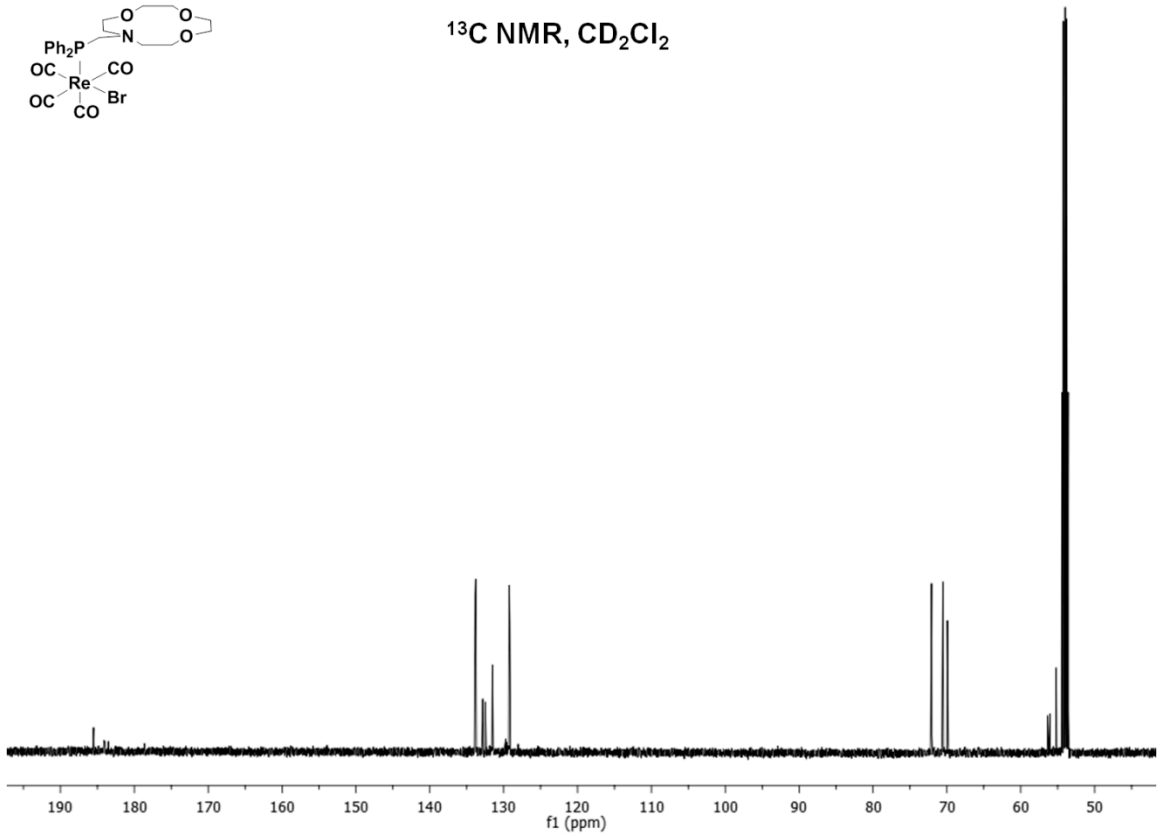

Figure S5. ^{13}C NMR spectrum of **3**.

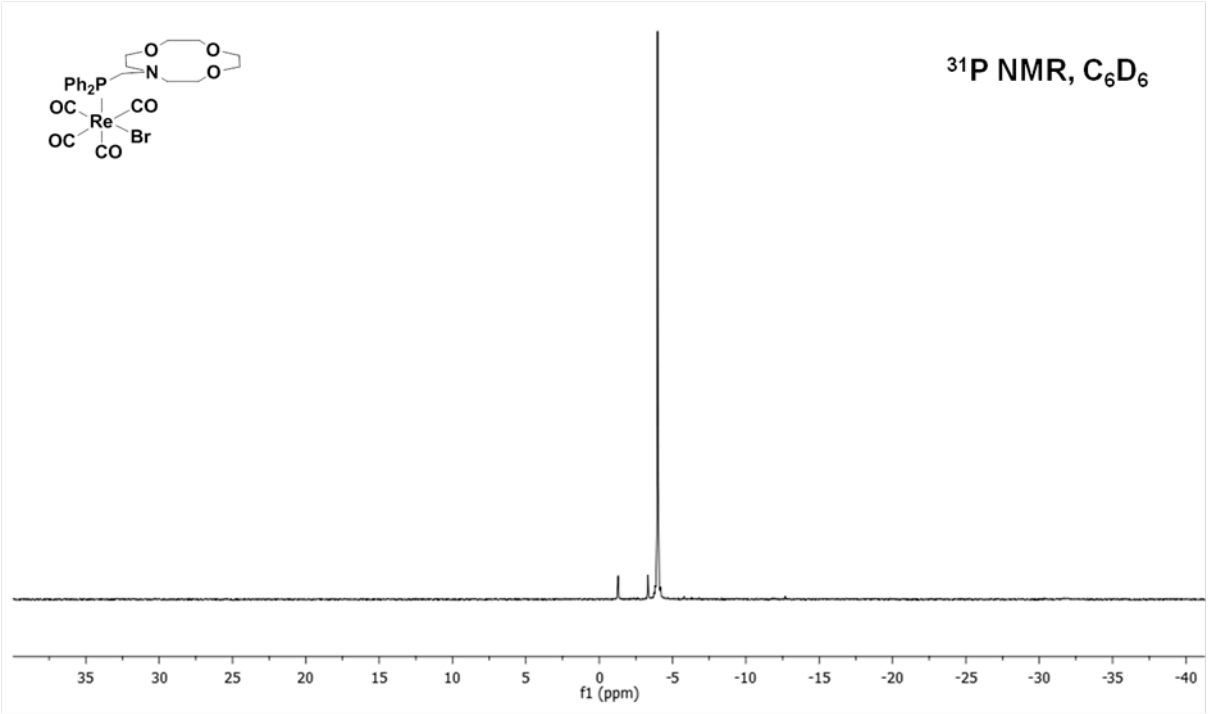

Figure S6. ^{31}P NMR spectrum of **3**.

[Re(CO)$_4$(PNO)][BF$_4$] (4). In the glovebox, a vial was charged with molecular sieves, **3** (500 mg, 0.662 mmol) and $AgBF_4$ (153.8 mg, 0.794 mmol), and CH_2Cl_2 (15 ml). Following stirring in the dark for 36 h, the suspension was filtered through celite and the filtrate evaporated *in vacuo*. The solid was recrystallized from CH_2Cl_2/Et_2O and dried *in vacuo* to afford a pale yellow crystalline solid (360 mg, 70%).

^{1}H NMR (500 MHz, CD_2Cl_2, δ, ppm): 7.82-7.75 (m, 4H), 7.67-7.62 (m, 6H), 5.90 (d, 2H, J = 5 Hz), 3.95-3.88 (m, 2H), 3.87-3.81 (m, 2H), 3.70-3.62 (m, 10H), 3.39 (dt, 2H, J = 5 Hz); ^{13}C NMR (125.7 MHz, CD_2Cl_2, δ, ppm): 187.1 (d, J = 8.8 Hz), 185.7 (d, J = 45.2 Hz), 184.4 (d, J = 6.3 Hz), 133.5 (d, J = 3 Hz), 132.5 (d, J = 12.6 Hz), 130.7 (d, J = 12.7 Hz), 127.7 (d, J = 53 Hz), 74.6 (d, J = 42.7 Hz), 71.2 (d, J = 40.2 Hz), 68.1, 67.4 (d, J = 6.2 Hz); ^{31}P NMR (121.5 MHz, CD_2Cl_2, δ, ppm): - 41.0 (s). IR (CH_2Cl_2, cm^{-1}): 2100, 2007, 1971, 1937. Elemental analysis $C_{25}H_{28}BF_4NO_7PRe•H_2O$: Calcd: C, 38.67; H, 3.89; N, 1.80. Found: C, 38.81; H, 4.01; N, 1.67.

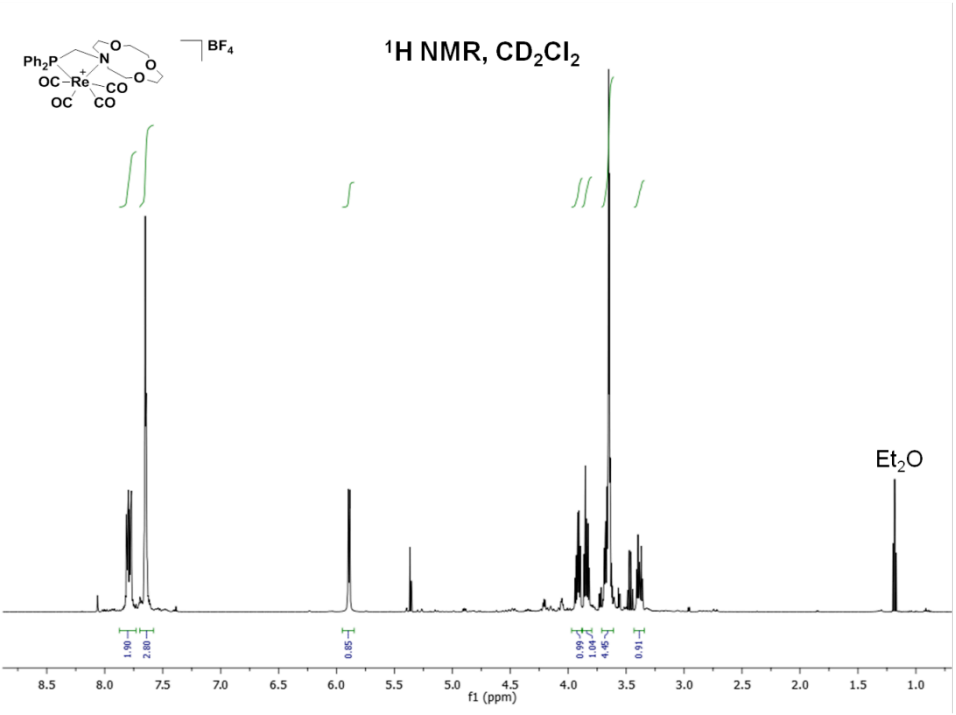

Figure S7. ^{1}H NMR spectrum of **4**.

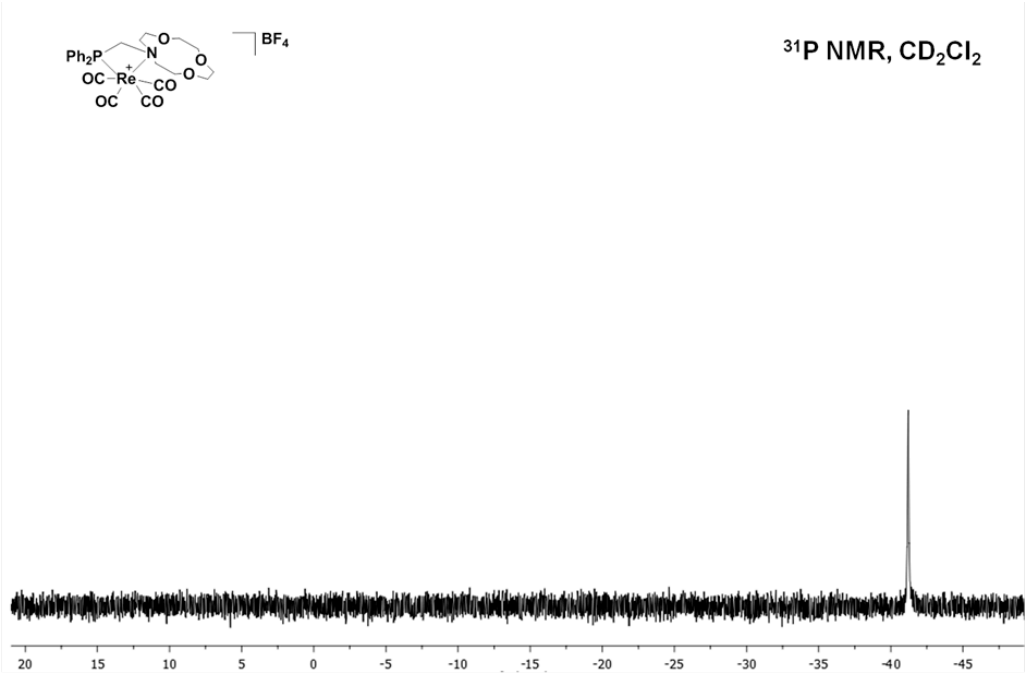

Figure S8. ^{31}P NMR spectrum of **4**.

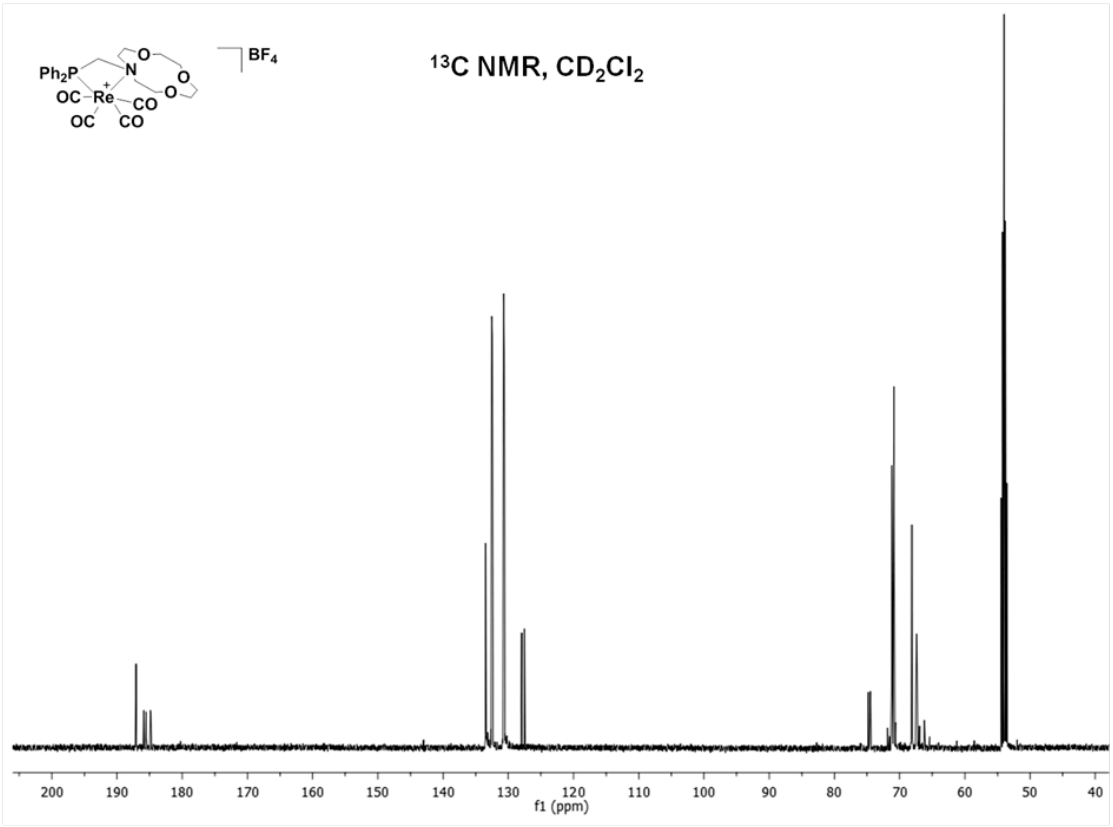

Figure S9. ^{13}C NMR spectrum of **4**.

[Re(CO)$_4$(PNO-ZnMe)Me][BF$_4$] (5). In the glovebox, $ZnMe_2$ (15 µl, 0.148 mmol) was added to a solution of **4** (100 mg, 0.124 mmol) in CH_2Cl_2 (5 ml) in a vial and stirred for 16 h. The solution was filtered and the filtrate was evaporated to a white solid. Colorless crystals of the product were grown from CH_2Cl_2/Et_2O (100 mg, 89%). ^{1}H NMR (500 MHz, CD_2Cl_2, δ, ppm): 7.74-7.64 (m, 4H), 7.61-7.56 (m, 6H), 4.07 (d, 2H, J = 5 Hz), 4.05-3.70 (m, 12H), 2.72 (t, 4H, J = 10 Hz), - 0.5 (d, 3H, J = 10 Hz), - 0.68 (s, 3H); ^{13}C NMR (125.7 MHz, CD_2Cl_2, δ, ppm): 191.9 (d, 10.1 Hz), 189.1 (d, 53 Hz), 187.9 (d, J = 10 Hz), 133.0 (d, J = 10 Hz), 132.4 (d, J = 2.5 Hz), 131.2 (d, J = 36.5), 130.2 (d, J = 10 Hz), 68.5, 66.2 (d, J = 41.5 Hz), 56.6 (d, J = 8.8 Hz), 51.8 (d, 2.5 Hz), - 18.2, - 32.1 (d, J = 8.8 Hz); ^{31}P NMR (121.5 MHz, CD_2Cl_2, δ, ppm): - 7.1 (s). IR (CH_2Cl_2, cm^{-1}): 2077, 1992, 1969, 1923. Elemental analysis $C_{27}H_{34}BF4NO_7PReZn$: Calcd: C, 37.97; H, 4.01; N, 1.64. Found: C, 37.89; H, 4.01; N, 1.69.

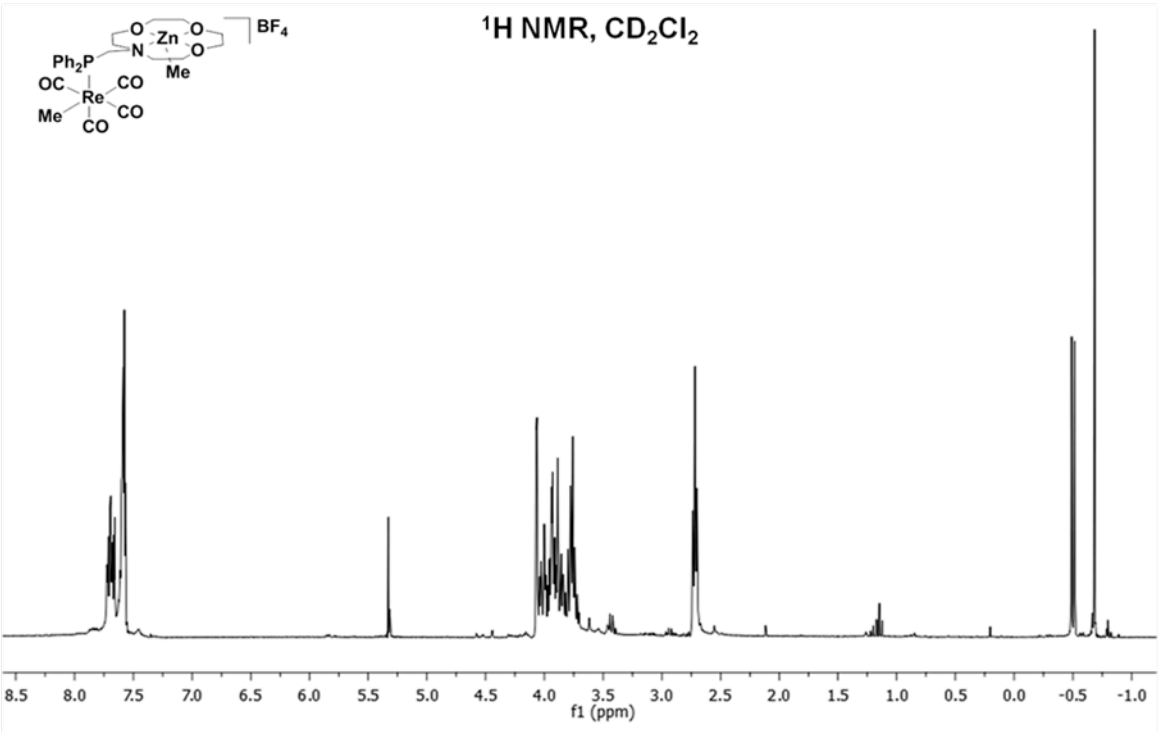

Figure S10. ^{1}H NMR spectrum of **5**.

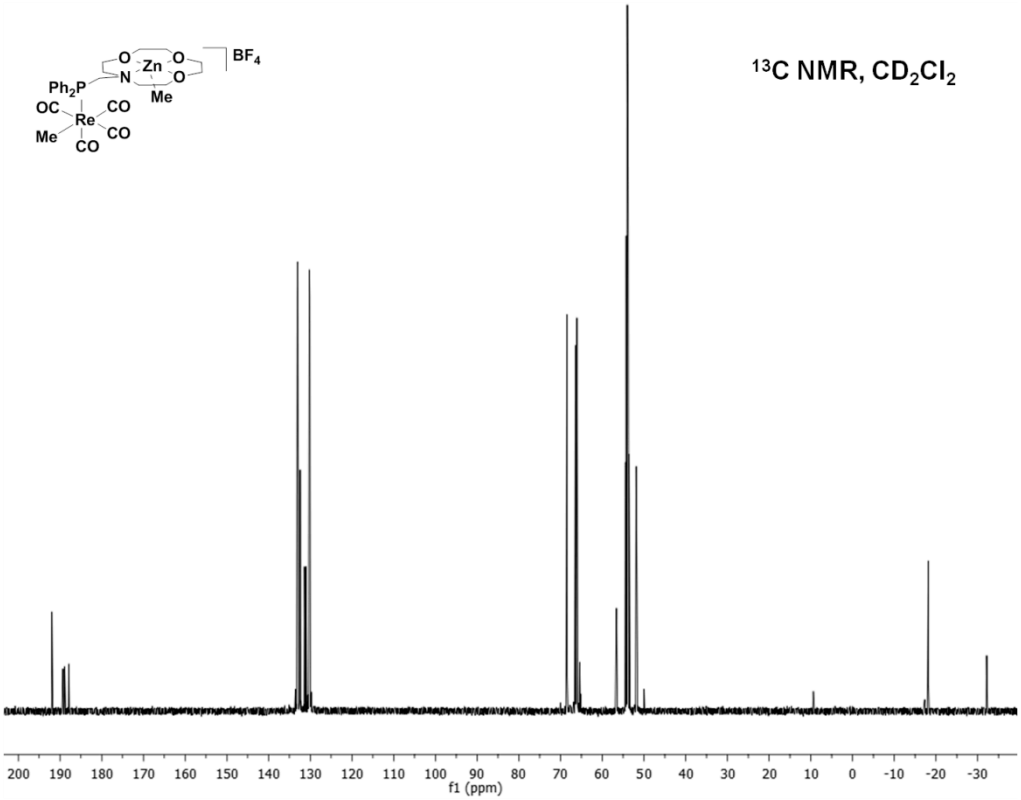

Figure S11. ^{13}C NMR spectrum of **5**.

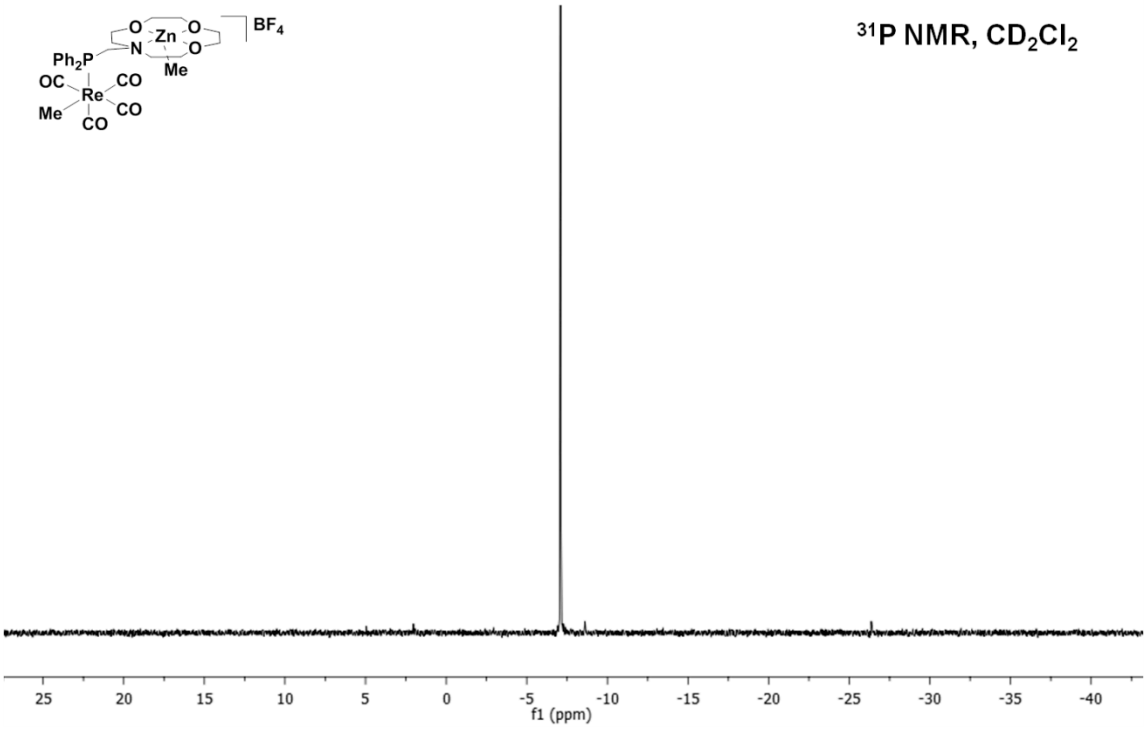

Figure S12. ^{31}P NMR spectrum of **5**.

[Re(CO)$_4$(PNO)Me] (6). In a vial, **5** (100 mg, 0.11 mmol) was dissolved in THF (2 ml) and the resulting solution passed through a pipette column of alumina (2 cm). The solvent was evaporated in *vacuo* and the residue washed with pentane and dried to afford **6** as a sticky white solid (60 mg, 79%). ^{1}H NMR (500 MHz, CD_2Cl_2, δ, ppm): 7.59-7.53 (m, 4H), 7.48-7.44 (m, 6H), 3.90 (d, 2H, J = 5 Hz), 3.57-3.54 (m, 4H), 3.48-3.45 (m, 4H), 3.44 (t, 4H, J = 5 Hz), 2.55 (t, 4H, J = 5 Hz); ^{13}C NMR (125.7 MHz, CD_2Cl_2, δ, ppm): 192.4 (d, J = 10 Hz), 190.3 (d, J = 51 Hz), 188.6 (d, J = 7.5 Hz), 133.7 (d, J = 8.8 Hz), 133.3 (d, J = 41.5 Hz), 130.9 (d, J = 2.5 Hz), 128.9 (d, J = 8.8 Hz), 72.1, 70.3 (d, J = 55.3), 58.3 (d, J = 36.5 Hz), 55.5 (d, J = 3.8 Hz), - 32.9 (d, J = 8.8 Hz); ^{31}P NMR (121.5 MHz, CD_2Cl_2, δ, ppm): 2.1 (s). IR (CH_2Cl_2, cm^{-1}): 2061, 1969, 1927. Elemental analysis $C_{26}H_{31}NO_7PRe$: Calcd: C, 45.47; H, 4.55; N, 2.04. Found: C, 41.48; H, 4.51; N, 2.01. **HRMS** (FAB$^+$): m/z calcd. for [$C_{26}H_{30}NO_7ReP$]: 686.1352. Found 686.1318 (M+H)-H_2, 672.1136 (M+H)-Me.

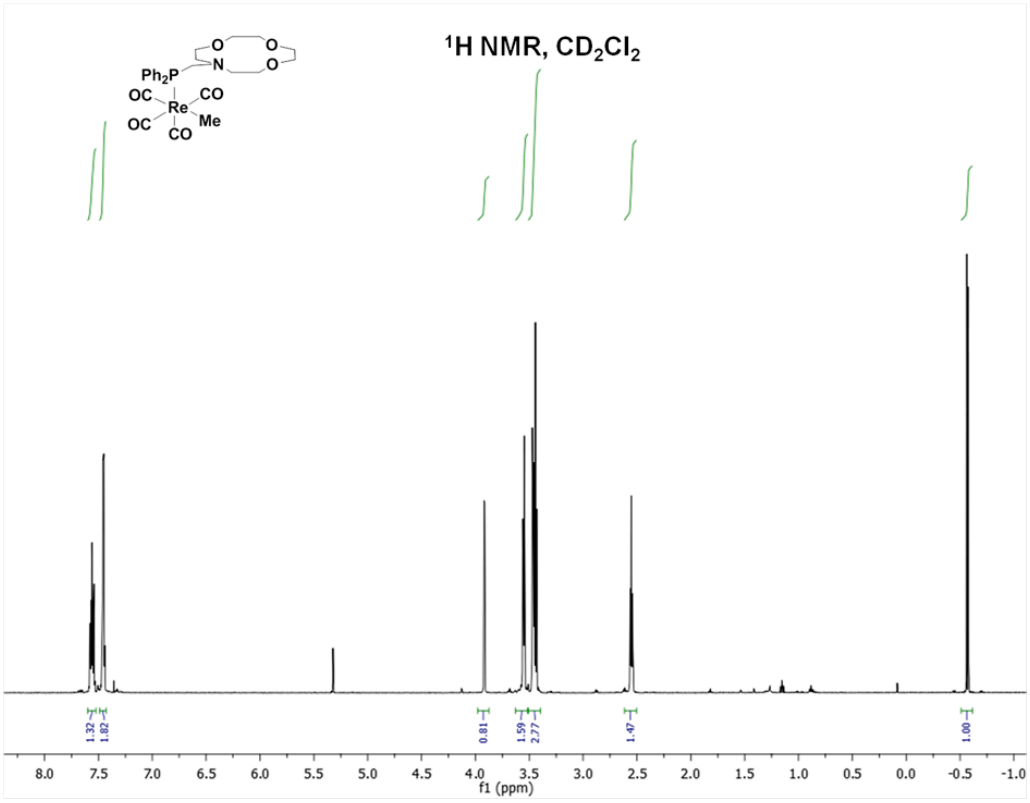

Figure S13. ^{1}H NMR spectrum of **6**.

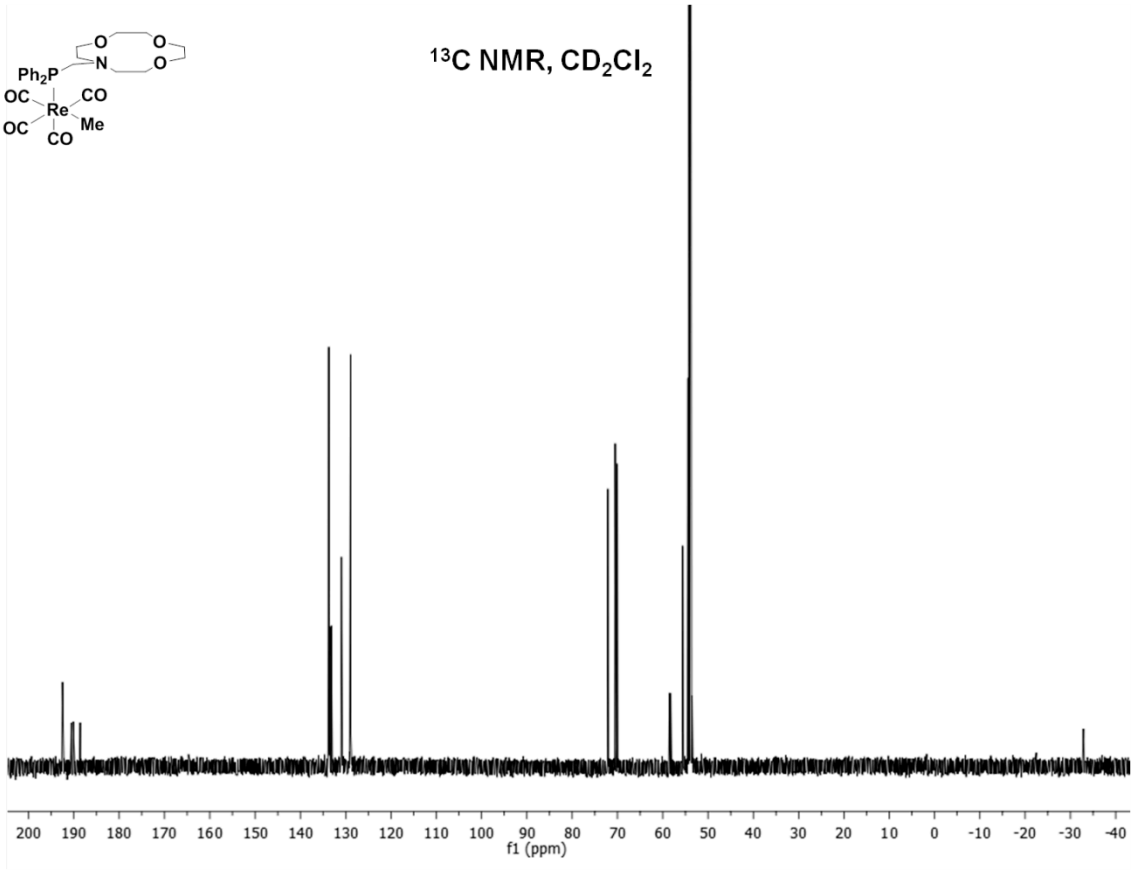

Figure S14. ^{13}C NMR spectrum of **6**.

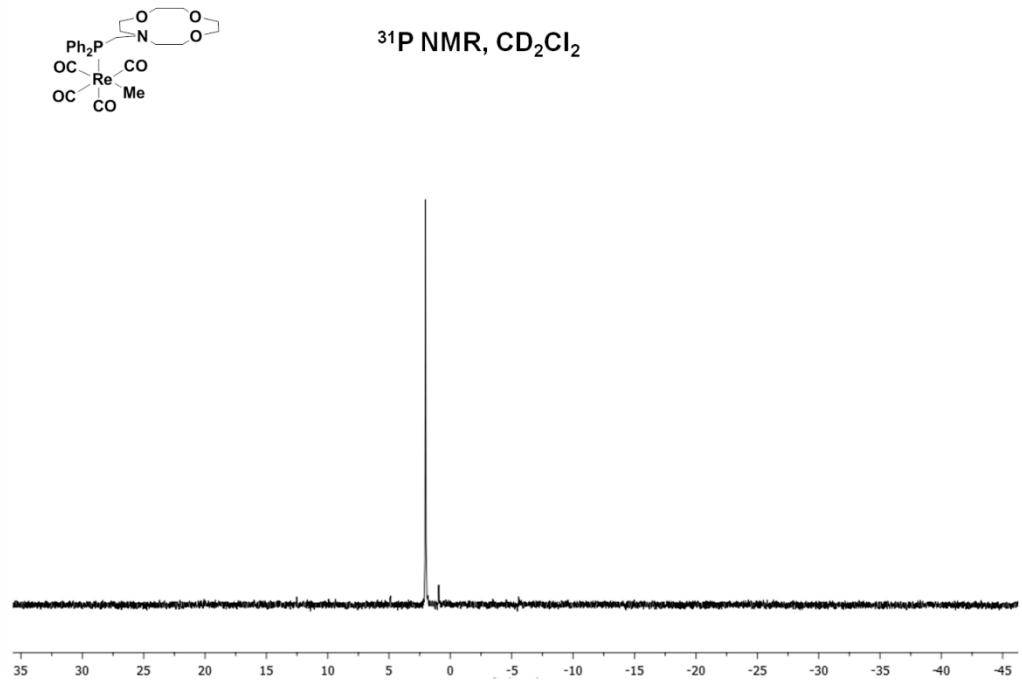

Figure S15. ^{31}P NMR spectrum of **6**.

S3 Migratory Insertion

General Procedure for NMR-Scale Addition of Lewis Acids to 6.

In the glovebox, the desired Lewis acid (0.029 mmol) was added to a J-Young NMR tube, followed by addition of a CD_2Cl_2 or CD_3CN (0.6 ml) solution of **6** (20 mg, 0.029 mmol). The tube was capped and inverted several times, until a homogeneous solution formed. The disappearance of **6** and appearance of migratory insertion products were monitored by ^{1}H and ^{31}P NMR. The ^{1}H and ^{13}C NMR spectra of both **8a** and **8b** are somewhat broadened at room temperature. Variable temperature NMR experiments did not lead to sharpening of the signals.

Reaction of 6 with $CaI_2(THF)_4$. $CaI_2(THF)_4$ (0.029 mmol, 16.7 mg) was added to the solution of **6**. **7a** was observed by NMR, but not isolated: ^{1}H NMR (500 MHz, CD_2Cl_2, δ, ppm): 7.80-7.71 (m, 4H), 7.56-7.45 (m, 6H), 5.03 (s br, 2H), 3.59-3.49 (m, 2H), 4.13-3.75 (4H, overlapping with THF), 3.23-3.08 (m, 2H), 2.67-2.55 (m, 2H), 0.56 (d, 3H, J = 7.5 Hz); ^{31}P NMR (121.5 MHz, CD_2Cl_2, δ, ppm): - 11.3.

Over 30 h, a pale yellow solution formed, concomitant with migratory insertion to form **8a**. Compound **8a** was precipitated by vapor diffusion of Et_2O into a CD_2Cl_2 solution to afford a white solid. The solids were dried *in vacuo*, but redissolution in CD_2Cl_2 was thwarted by poor solubility. The addition of a drop of THF to the CD_2Cl_2 suspension led to a homogeneous solution. Spectroscopic data were consistent with those recorded *in situ*: ^{1}H NMR (500 MHz, CD_2Cl_2, δ, ppm); 7.70-7.59 (br m), 7.50-7.40 (br m), 7.38-7.43 (br m), 4.42-4.31 (br m), 4.27-4.08 (br m), 4.04-3.80 (br m), 3.58-3.53 (br m), 3.48-3.43 (br m), 2.92-2.78 (br m), 2.75-2.68 (br m), 2.73 (s, overlapping), 2.59-2.55 (br m), 2.44-2.39 (br m); ^{13}C NMR (125.7 MHz, CD_2Cl_2, δ, ppm); 299.4 (d, J = 8.8 Hz), 192.5 (d, J = 61.8 Hz), 191.7 (d, J = 7.2 Hz), 191.1 (d, J = 6.2 Hz), 133.8 (d, J = 8.8 Hz), 133.0 (br m), 131.2 (d, J = 6.3 Hz) 129.3 (d, J = 2.5

Hz), 129.2 (d, J = 2.5 Hz), 69.2 (d, J = 45.3), 68.9, 67.7 (d, J = 39.0 Hz), 61.8 (d, J = 24.6 Hz), 56.1 (br m), 55.7; ^{31}P NMR (121.5 MHz, CD_2Cl_2, δ, ppm): - 10.8 (s). IR (CD_2Cl_2, cm^{-1}): 2021, 1942, 1896.

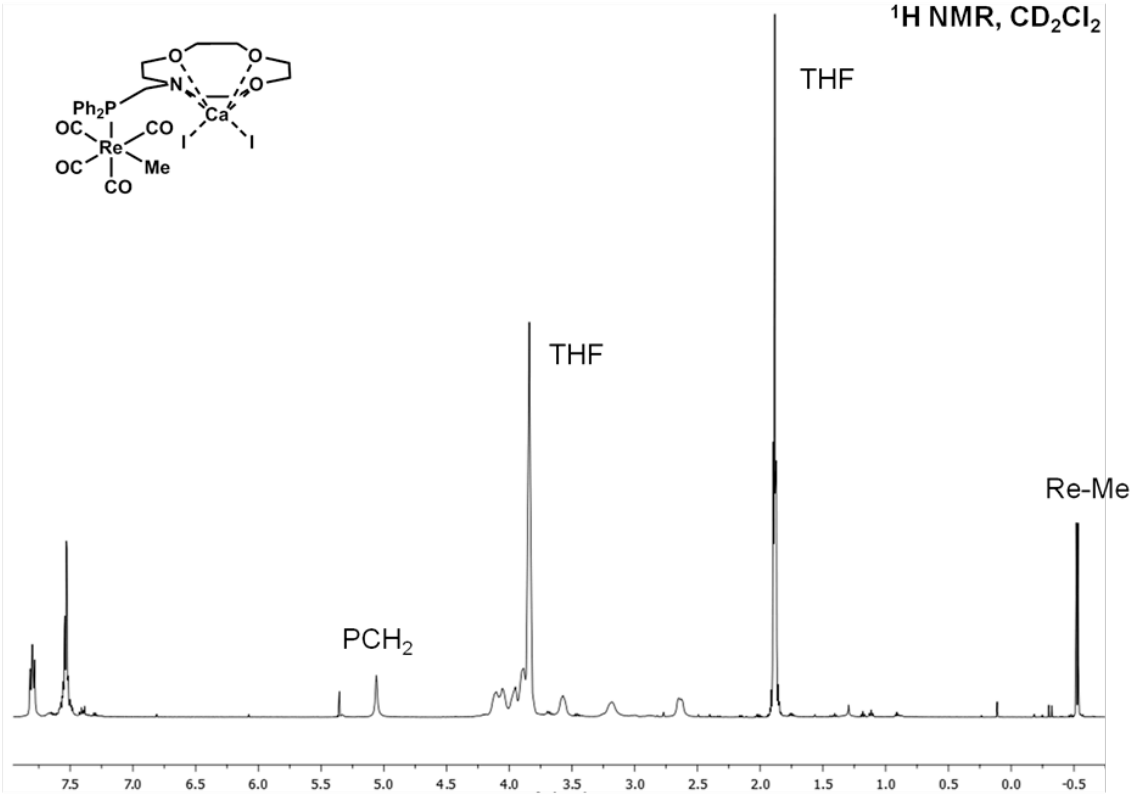

Figure S16. ^{1}H NMR spectrum of **7a**.

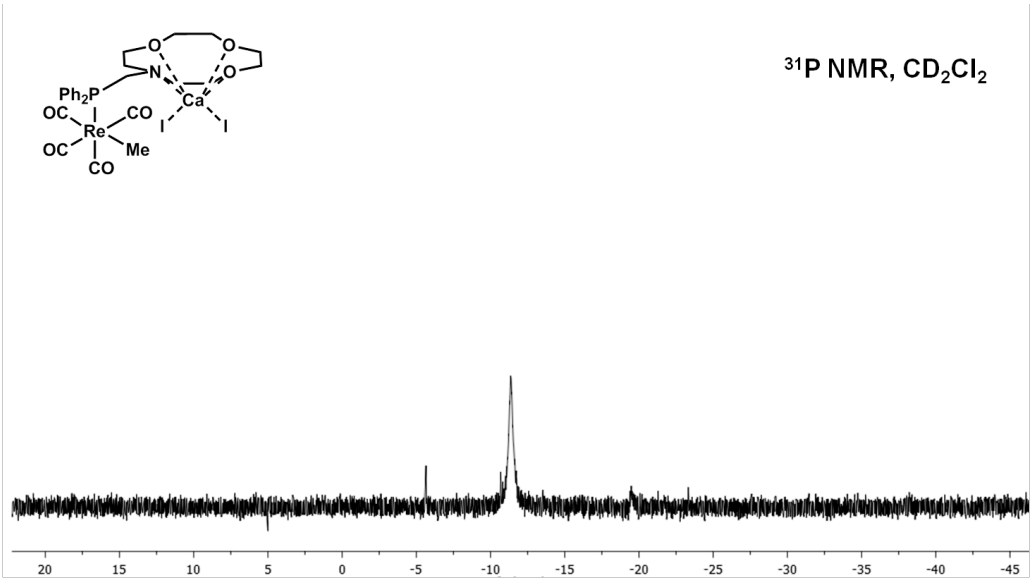

Figure S17. ^{31}P NMR spectrum of **7a**.

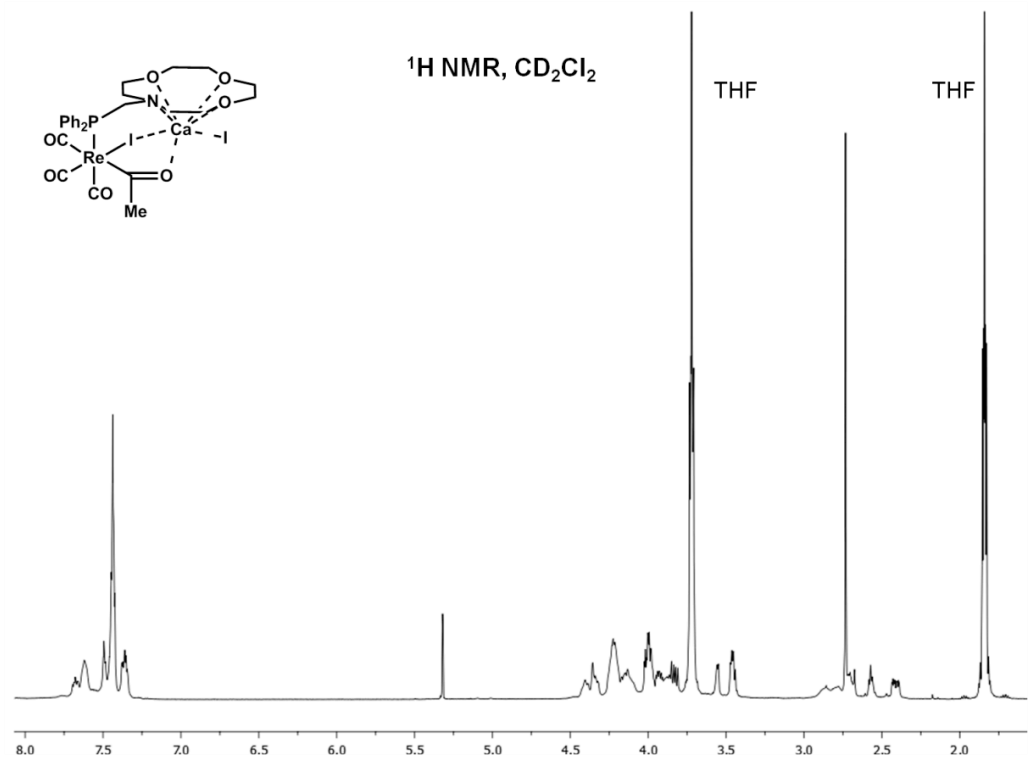

Figure S18. ^{1}H NMR spectrum of **8a**.

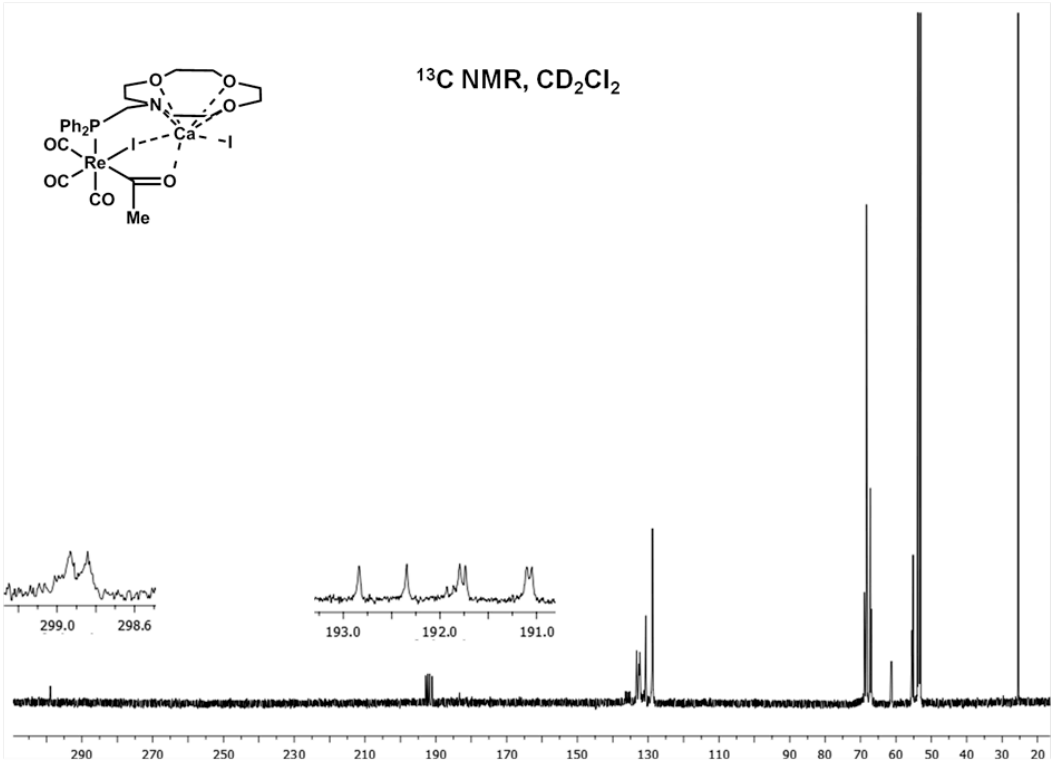

Figure S19. ^{13}C NMR spectrum of **8a**.

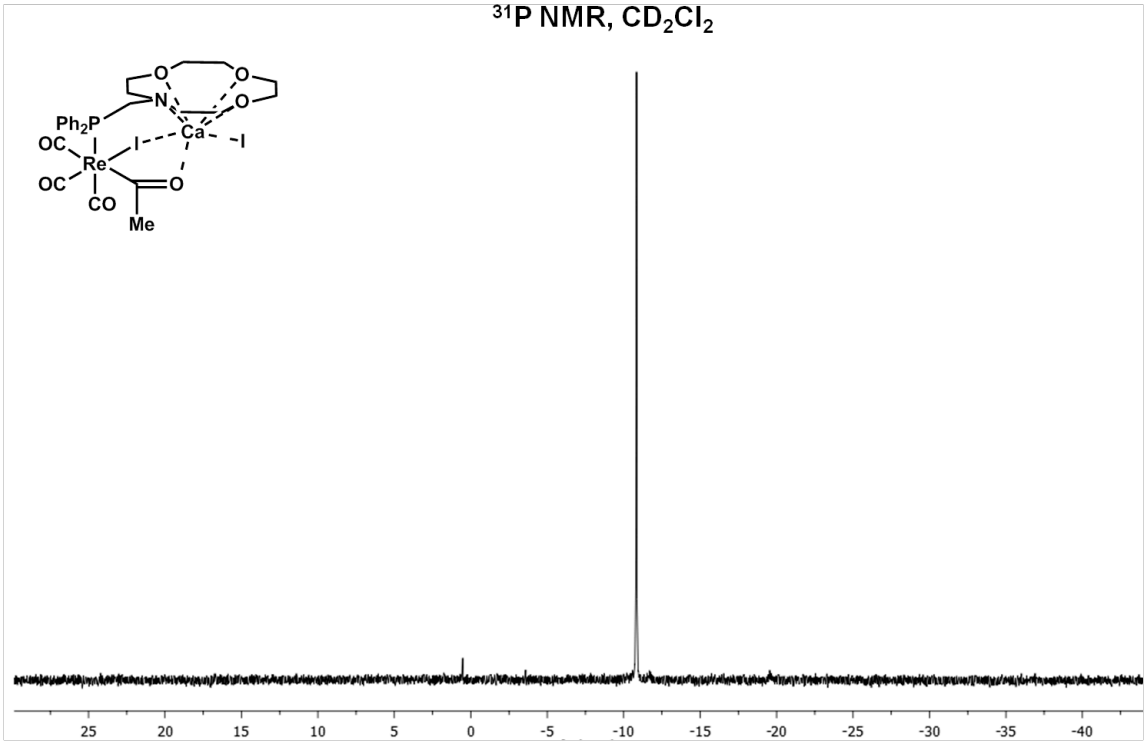

Figure S20. ^{31}P NMR spectrum of **8a**.

Reaction of 6 with $SrI_2(THF)_5$. $SrI_2(THF)_5$ (0.029 mmol, 20.2 mg) was added to the solution of **6**. **7b** was observed by NMR, but not isolated. **7b.** ^{1}H NMR (300 MHz, CD_3CN, δ, ppm); 7.82-7.75 (m, 4H), 7.56-7.53 (m, 6H), 4.66 (d, 2H, J = 3 Hz), 3.80-3.70 (br m), 3.67-3.58 (br m, overlapping with THF), 2.61 (t, 4H, J = 6 Hz), - 0.59 (d, 3H, J = 6 Hz); ^{31}P NMR (121.5 MHz, CD_2Cl_2, δ, ppm): - 9.5 (s).

During the course of the reaction (~ 24 h), **8b** precipitated. The reaction was monitored by ^{1}H NMR and judged to be complete by following the disappearance of the signal corresponding to the Re-Me protons at – 0.59 ppm. The supernatant was then removed and the residue taken up in CD_3CN. ^{1}H NMR (500 MHz, CD_3CN, δ, ppm); 7.57-7.47 (m, 7H) 7.47-7.39 (m, 3H), 4.61-4.51 (dd, 1H, J = 15 Hz, J = 10 Hz), 4.34-4.25 (br m, 1H), 4.13-3.66 (br m, 11H), 3.89-3.85 (dd, 1H, J = 15 Hz, J = 10 Hz, overlapping), 3.62-3.54 (br m, 1H), 2.88-2.79 (br m, 1H), 2.75 (s, 3H), 2.58-2.50 (br m, 1H), 2.43-2.33 (br m, 1H), 2.24-2.16 (br m, 1H); ^{13}C NMR (125 MHz, CD_3CN, δ, ppm); 294.5 (d, J = 12.4 Hz), 194.0 (d, J = 62.5 Hz), 193.3 (d, J = 7.5 Hz), 192.2 (d, J

= 7.5 Hz), 133.5 (br m), 131.6 (br m), 130.9, 128.4 (d, J = 8.8 Hz), 128.3 (d, J = 8.8 Hz), 67.7 (d, J = 11.2 Hz), 67.3 (br) 66.5 (d, J = 28.8 Hz) 61.2 (d, J = 25 Hz), 55.0-54.6 (br, m); ^{31}P NMR (121.5 MHz, CD_2Cl_2, δ, ppm): - 12.7 (s). IR (CD_3CN, cm^{-1}): 2015, 1930, 1887.

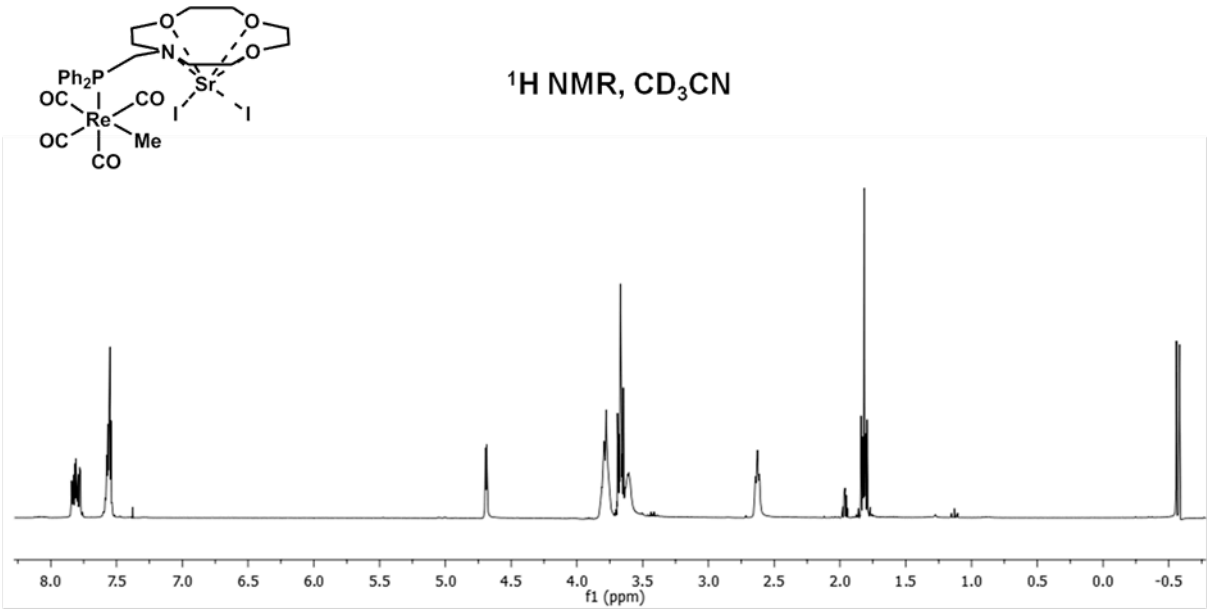

Figure S21. ^{1}H NMR spectrum of **7b**.

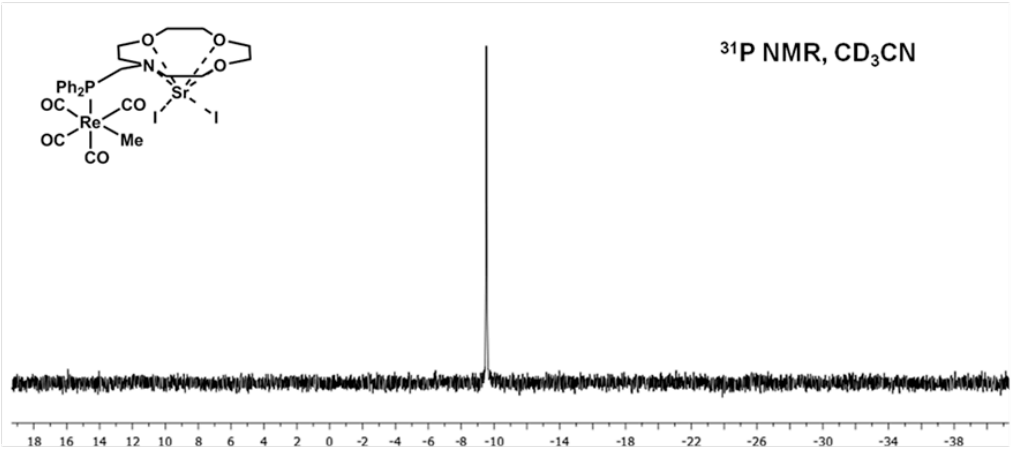

Figure S22. ^{31}P NMR spectrum of **7b**.

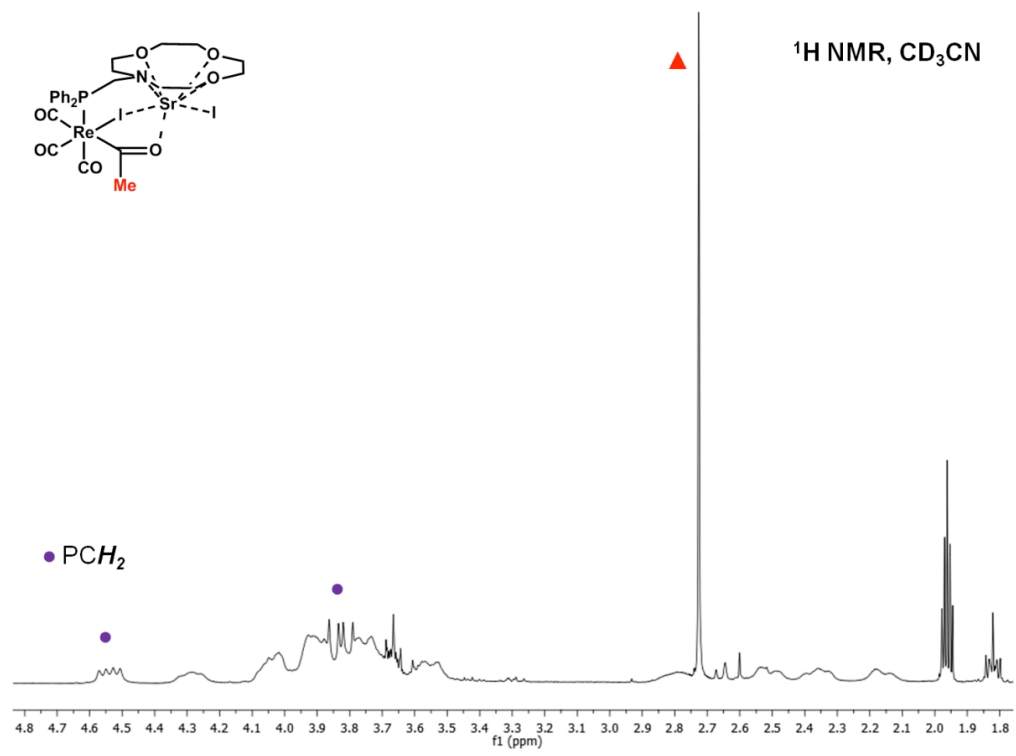

Figure S23. ^{1}H NMR spectrum of **8b**.

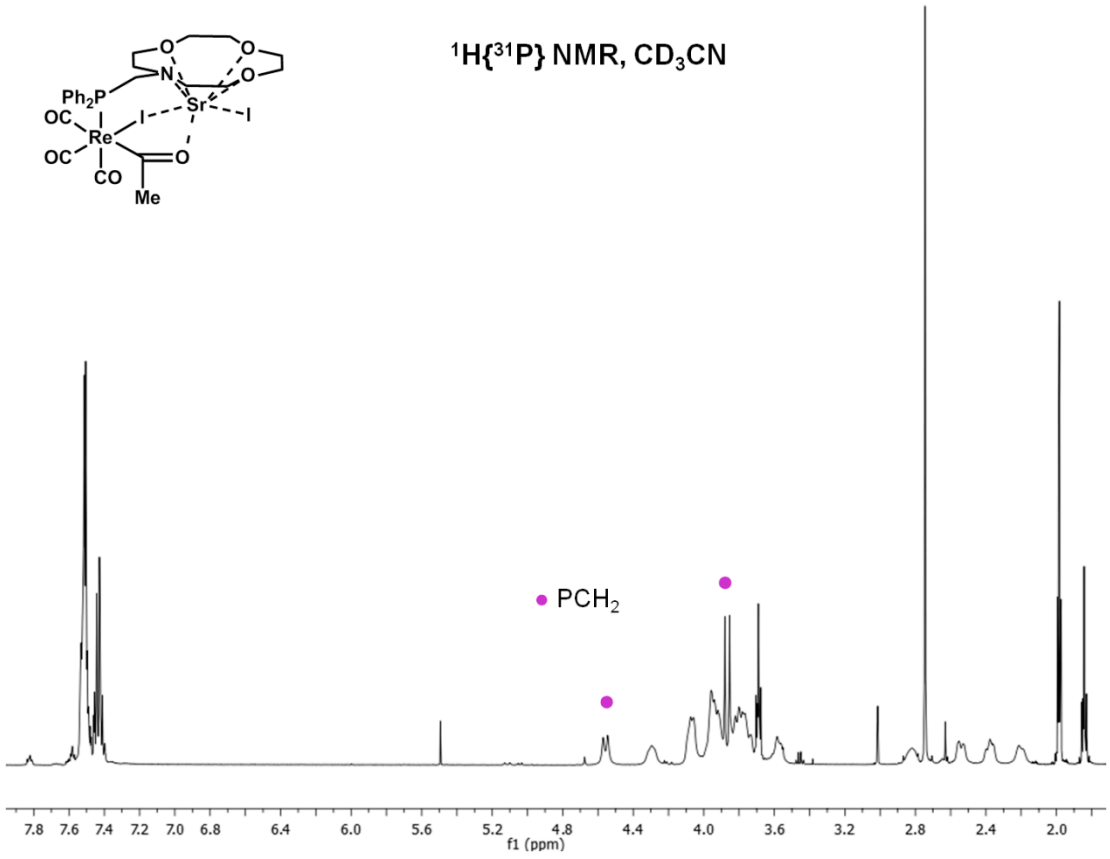

Figure S24. ^{1}H{^{31}P} NMR spectrum of **8b**.

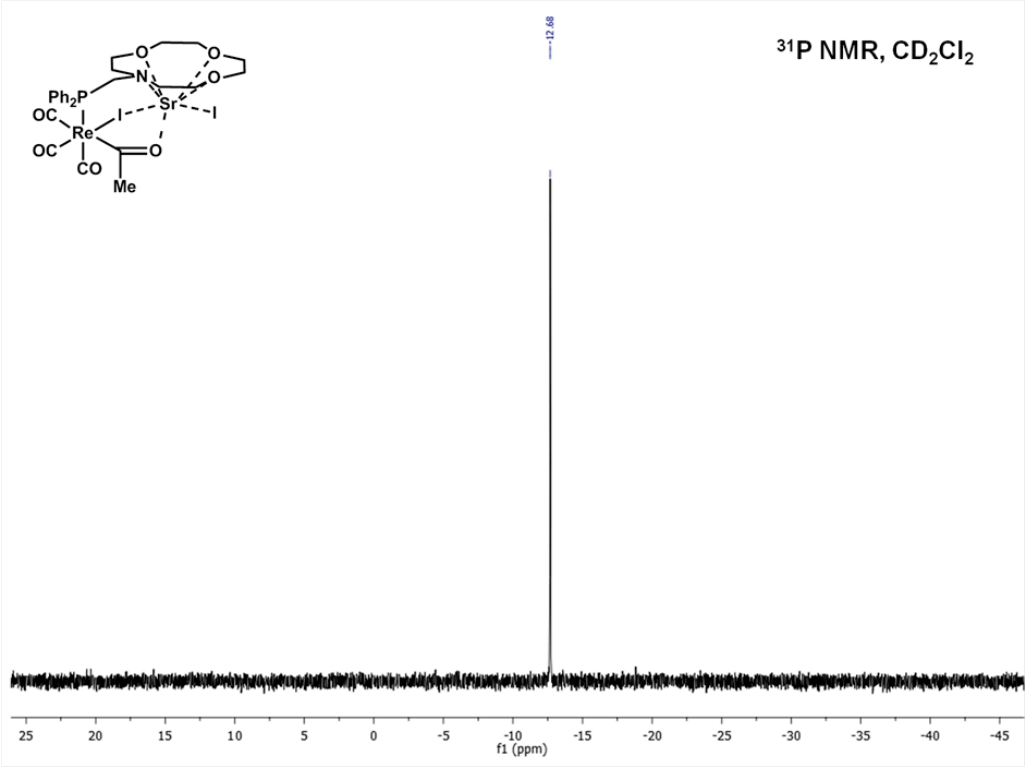

Figure S25. ^{31}P NMR spectrum of **8b**.

Reactions of 6 with $MgX_2(THF)_n$. $MgX_2(THF)_n$ (0.029 mmol, X = Br, Cl or I) was added to the solution of **6**. The reactions were monitored by ^{1}H and ^{31}P NMR spectroscopy for a period of 14 days but failed to proceed to completion. Heating the reaction mixture to 40 °C led to the formation of by-products.

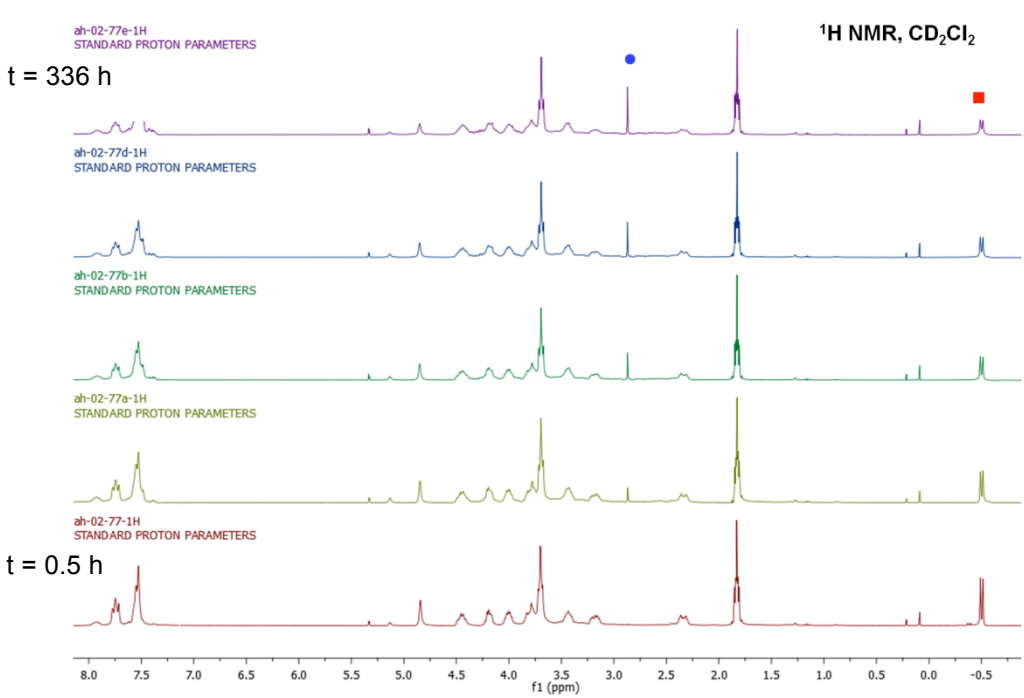

Figure S26. ^{1}H NMR spectrum showing the progression of the reaction of **6** with $MgBr_2(THF)_4$. A characteristic resonance for the acyl protons at 2.7 ppm grows in over a period of 14 days, concomitant with a decrease in the intensity of the resonance for the Re-Me protons.

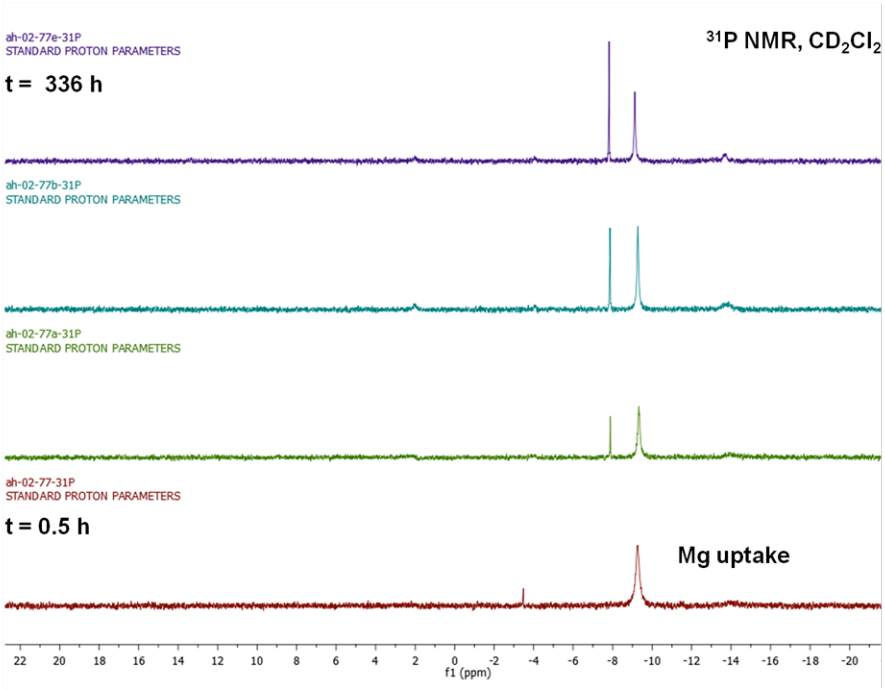

Figure S27. ^{31}P NMR spectrum showing the progression of the reaction of **6** with $MgBr_2(THF)_4$. Uptake of Mg^{2+} into the macrocycle is evidenced by a single broad peak at -9.2 ppm, shifted upfield by 11 ppm from **6**. The new peak growing in at -8 ppm is suggestive of the formation of the migratory insertion product.

Reaction of 6 with $CaI_2(THF)_4$ in CD_3CN. $CaI_2(THF)_4$ (0.029 mmol, 16.7 mg) was added to a solution of **6** (0.029 mmol) in 0.6 ml CD_3CN. The reaction was monitored by ^1H and ^{31}P NMR spectroscopy over a period of 7 days. Formation of the migratory insertion product **8a** was observed.

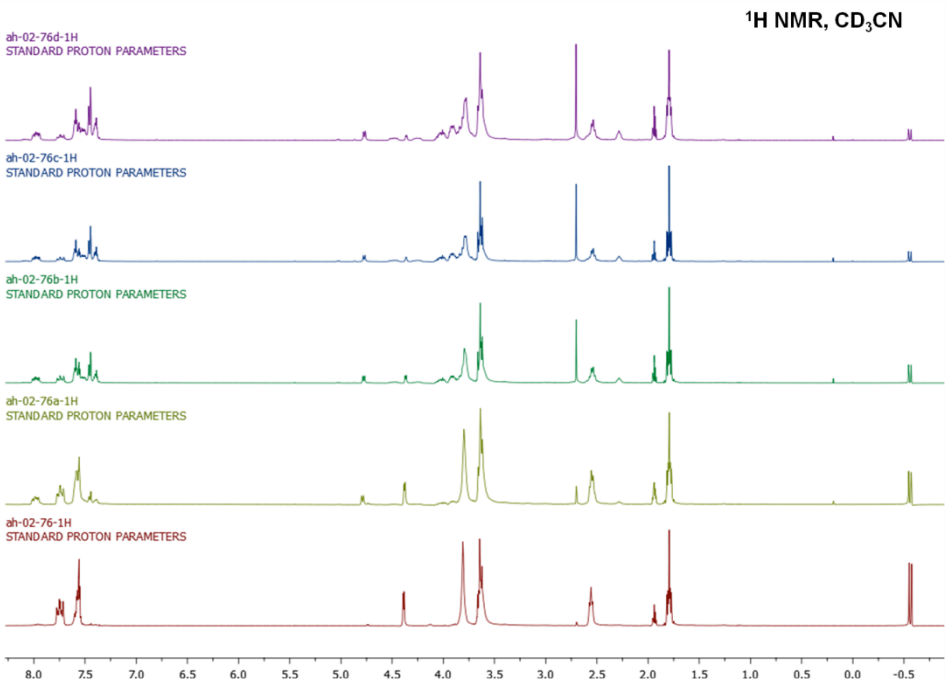

Figure S28. ^1H NMR spectrum showing the progression of the reaction of **6** with $CaI_2(THF)_4$ in CD_3CN (bottom to top).

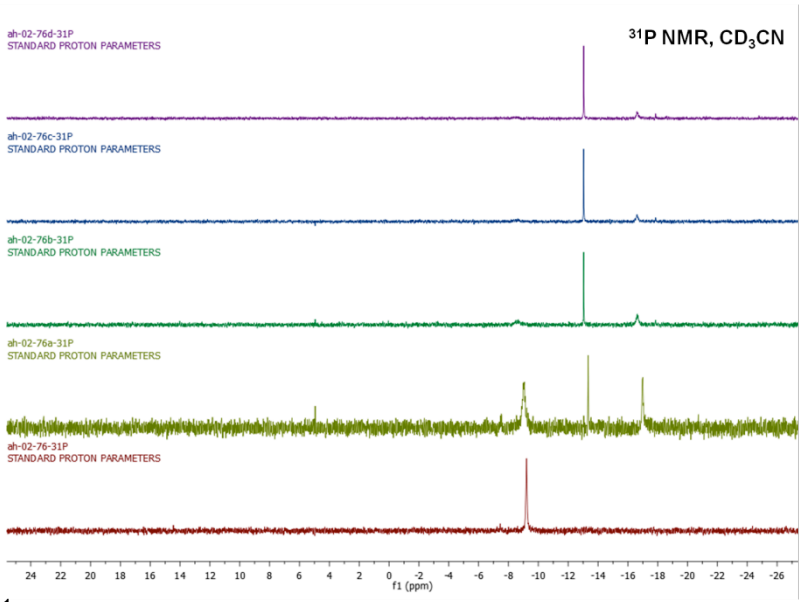

Figure S29. ^{31}P NMR spectrum showing the progression of the reaction of **6** with $CaI_2(THF)_4$ in CD_3CN (bottom to top).

S4: Reactivity Studies

Complexes **8a** and **8b** were generated *in situ* for reactivity studies.

Reaction of 8a with 12-crown-4

Following quantitative formation of the migratory insertion product **8a**, as assessed by ^{1}H and ^{31}P NMR, 1 equivalent of 12-crown-4 (5 mg, 0.029 mmol) as a stock solution in THF was added to the J-Young NMR tube containing **8a**. Monitoring of the reaction by NMR spectroscopy showed rapid de-insertion resulting in the formation of **6**.

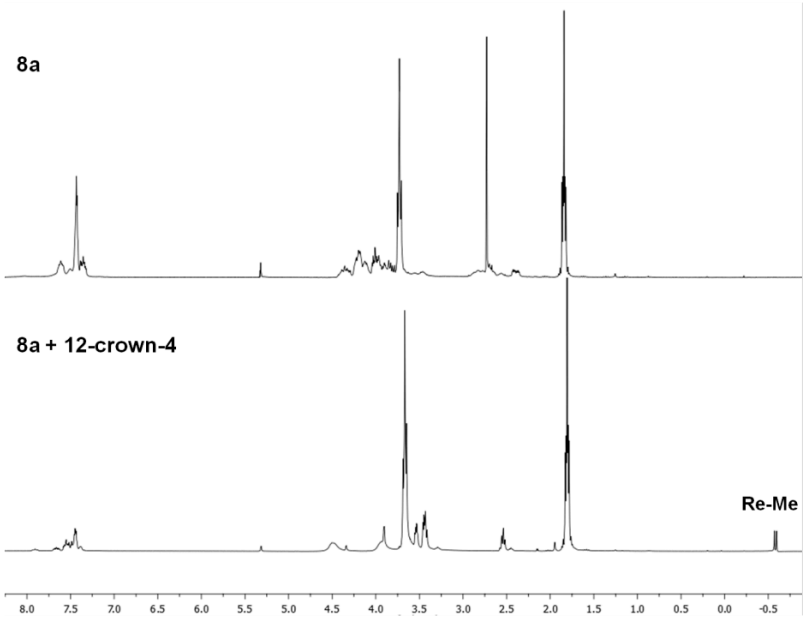

Figure S30. ^{1}H NMR spectrum (CD_2Cl_2) of the reaction of **8a** with 12-crown-4.

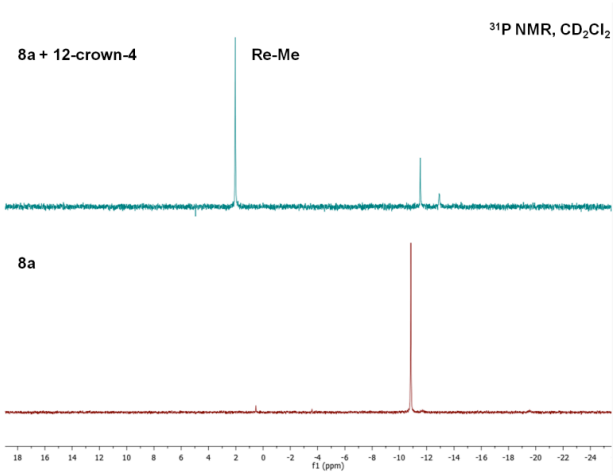

Figure S31. ^{31}P NMR spectrum of the reaction of **8a** with 12-crown-4.

Reaction of 8a with PMe_3 and 12-crown-4

5 µL PMe_3 (0.0516 mmol, 1.2 equiv) was added to a J-Young NMR tube containing **8a** (42 mg, 0.043 mmol) in CD_2Cl_2, and a ^{31}P NMR spectrum was recorded. After 1 h 12-crown-4 (0.043 mmol, 1 equiv) was added by syringe resulting in the formation of a white precipitate. The tube was returned to the glove box and the precipitate filtered off. Analysis of the solution by ^{31}P NMR showed two doublets at – 42.7 and 5.5 ppm (J_{PP} = 30 Hz). The ^{1}H NMR spectrum showed characteristic resonances for the acyl and PMe_3 protons at 2.34 and 1.11 ppm respectively. Isolation of **9** was precluded by its instability, decomposing to a complex mixture of products over 12 h. IR (CD_2Cl_2, cm^{-1}): 2006, 1968, 1914, 1567.

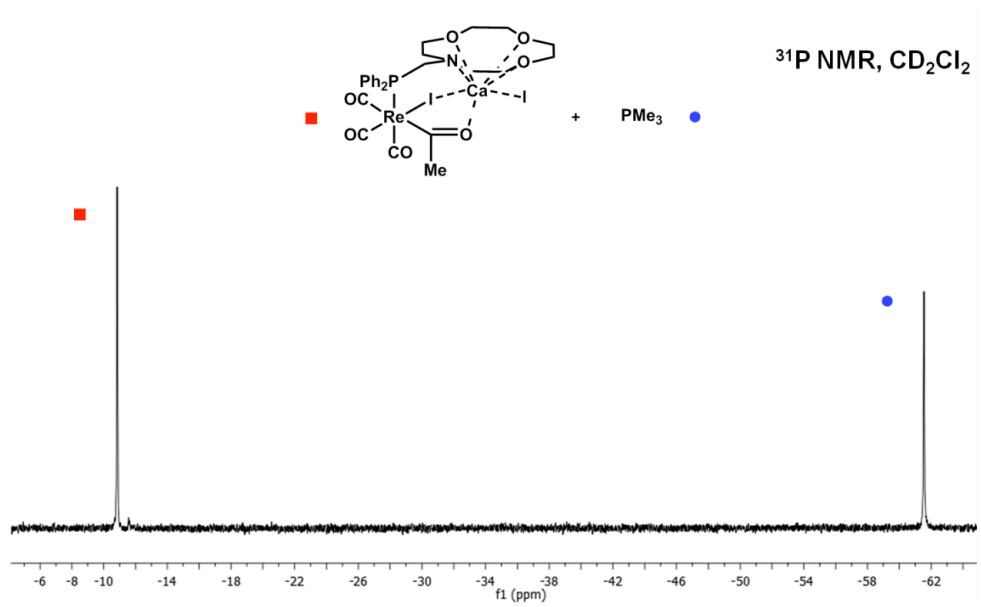

Figure S32. ^{31}P NMR spectrum immediately following the addition of PMe_3 to **8a**.

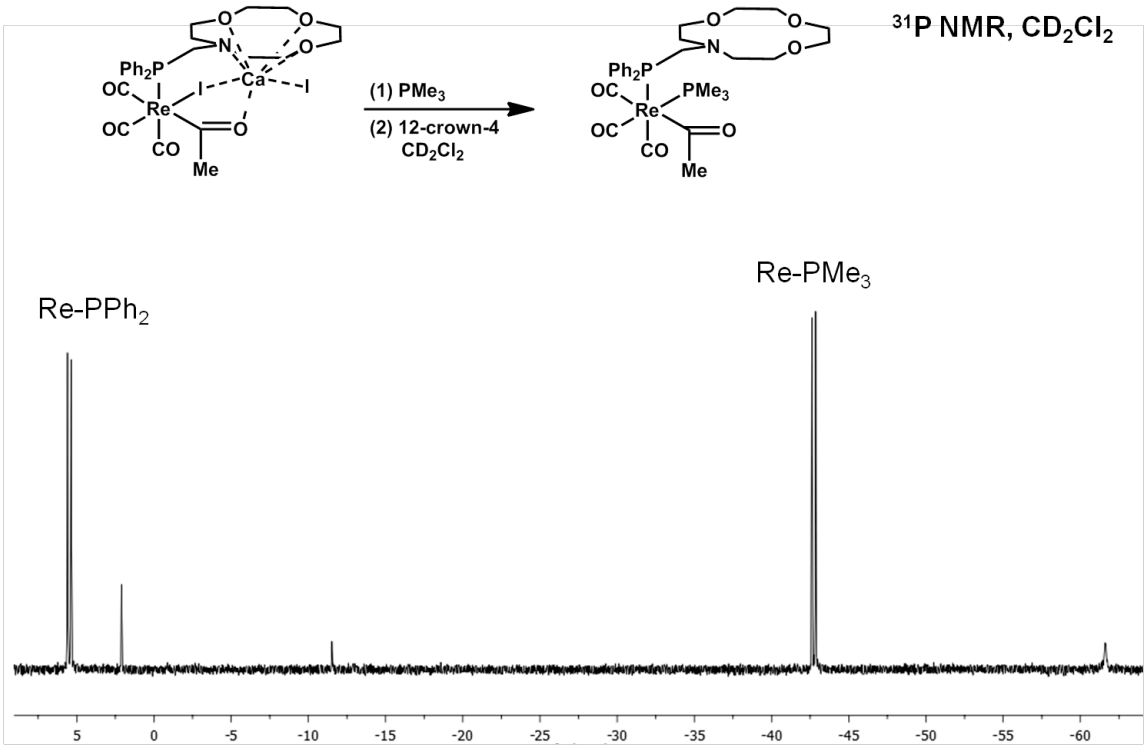

Figure S33. ^{31}P NMR spectrum of **9**.

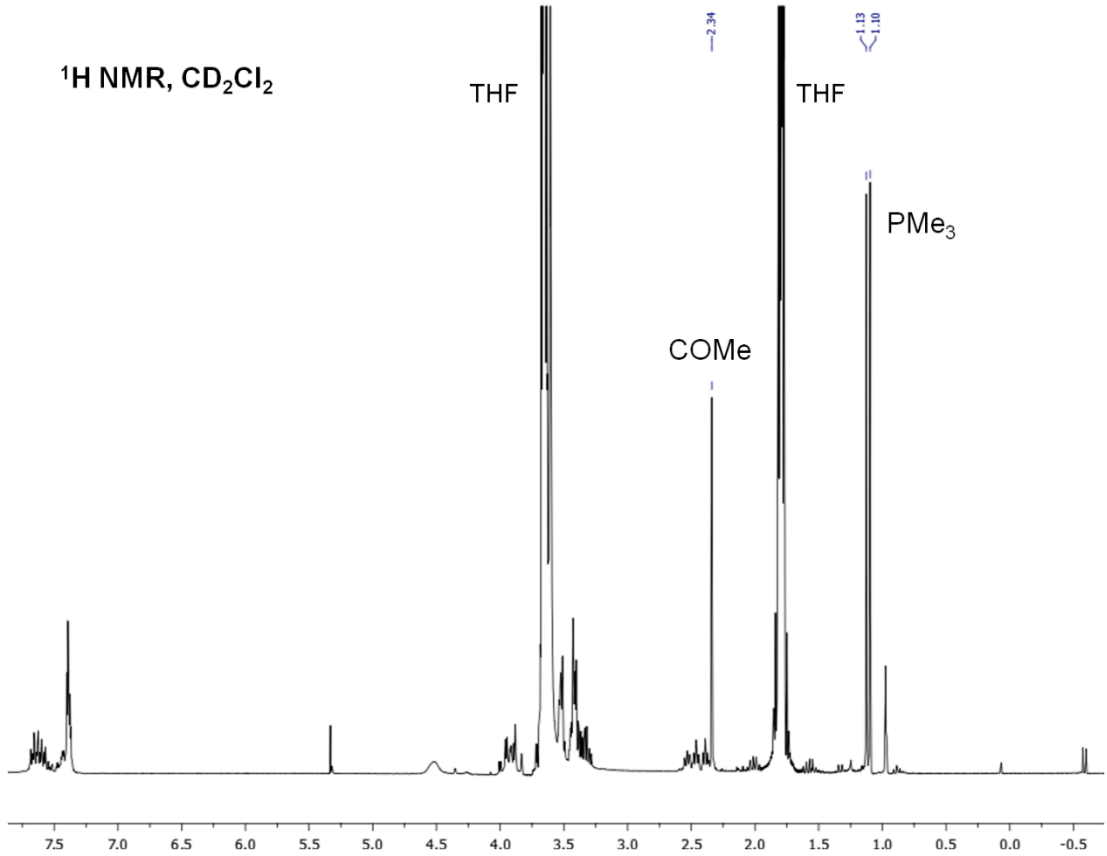

Figure S34. ^{1}H NMR spectrum of **9**.

Reaction of 8a with H_2O

Following quantitative formation of the migratory insertion product **8a**, as assessed by ^{1}H and ^{31}P NMR, 5 µl of H_2O (~ 5 equiv) was added to the J-Young NMR tube containing **8a**. The tube was capped and inverted several times. The reaction was monitored by ^{1}H and ^{31}P NMR spectroscopy over a period of 24 h. After this period, the volatiles were vacuum transferred to a second J-Young NMR tube and a ^{1}H NMR spectrum was recorded.

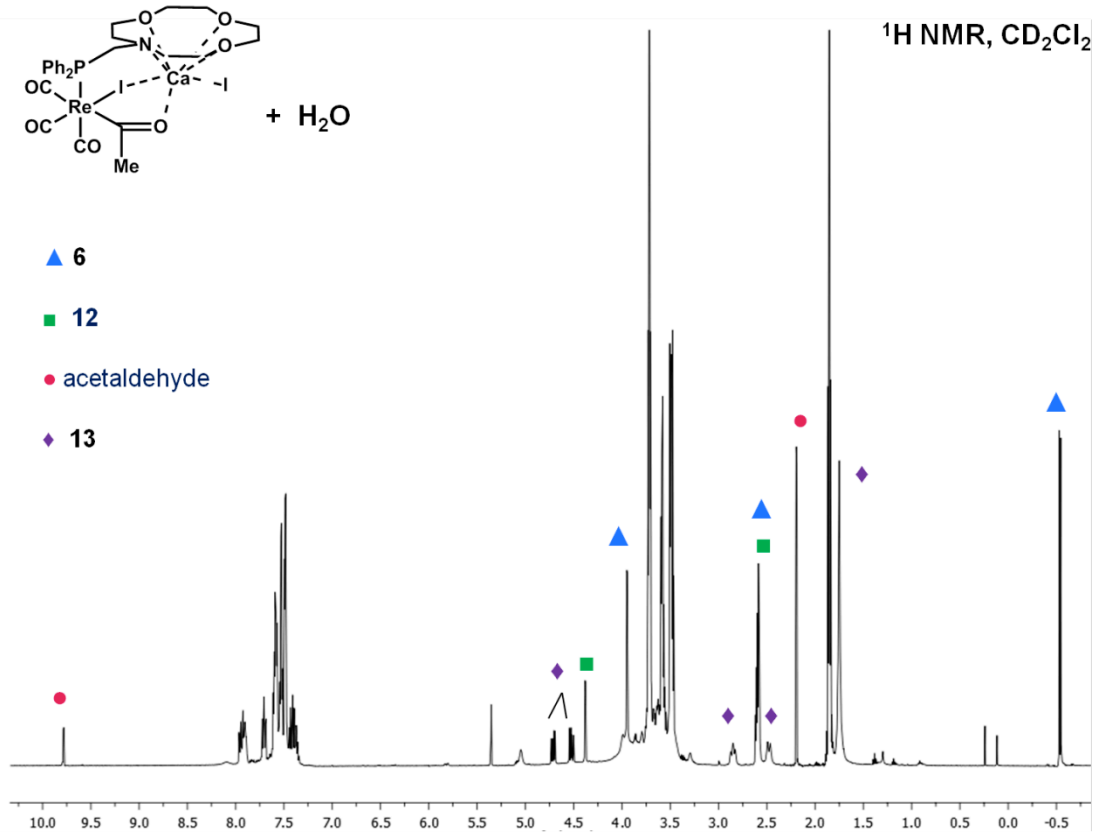

Figure S35. ^{1}H NMR of reaction mixture after 24 h.

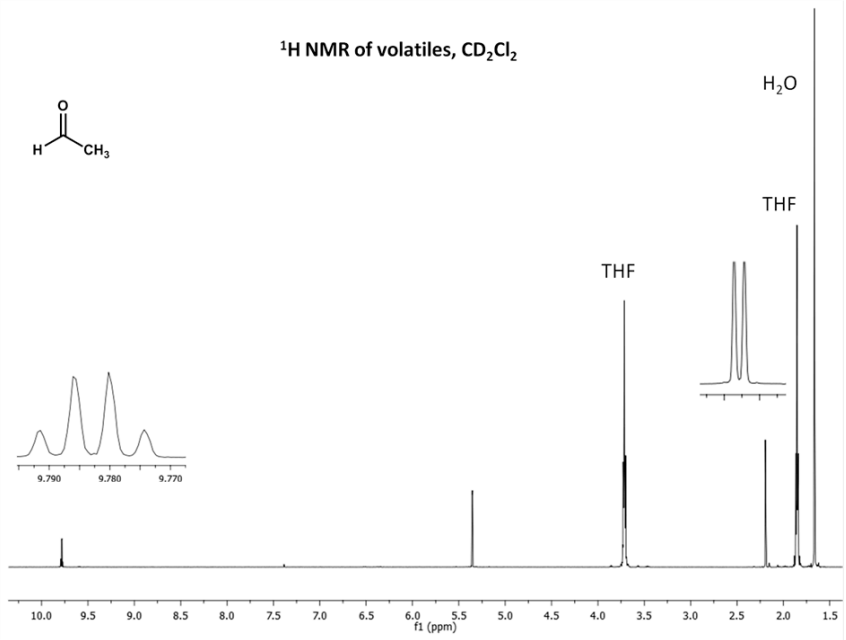

Figure S36. ^{1}H NMR spectrum of volatiles.

Following quantitative formation of the migratory insertion product **8a**, as assessed by ^{1}H and ^{31}P NMR, 50 µl of H_2O (~ 50 equiv) was added to the J-Young NMR tube containing **8a**. The tube was capped and inverted several times. The reaction was monitored by ^{1}H and ^{31}P NMR spectroscopy over a period of 24 h. Formation of complex **13** was observed immediately after the addition of water. **13** underwent de-insertion to complex **6** over a period of several hours. Crystals of **13** suitable for X-ray diffraction were obtained from the addition of 5 µl of H_2O to a sample of **8a**.

^{1}H NMR (500 MHz, CD_2Cl_2, δ, ppm); 7.96-7.87 (br m, 2H), 7.62-7.46 (br m, 4H), 7.36-7.29 (br m, 2H), 4.13 (dd, J = 15 Hz, J = 10 Hz), 3.98-3.88 (br m), 3.91 (dd, J = 15 Hz, J = 10 Hz, overlapping), 3.75-3.45 (br m, overlapping with THF), 3.12 (br m, 2H), 2.33 (br m, 2H), 1.76; ^{13}C NMR (125.7 MHz, CD_2Cl_2, δ, ppm); 287.9 (d, J = 10.5 Hz), 199.4 (d, J = 8.1 Hz), 197.0 (d, J = 8.8 Hz), 194.1 (d, J = 59.6 Hz), 135.0 (d, J = 47.5 Hz), 134.0 (d, J = 11.2 Hz), 130.6 (d, J = 10 Hz), 129.1 (d, J = 9.9 Hz) 128.9 (d, J = 10.4 Hz), 128.7 (d, J = 2.5 Hz), 70.9, 70.2, 68.2, 56.7 (d, J = 7.5 Hz), 54.1 (d, J = 30 Hz), 48.6; ^{31}P NMR (121.5 MHz, CD_2Cl_2, δ, ppm): 7.1 (s).

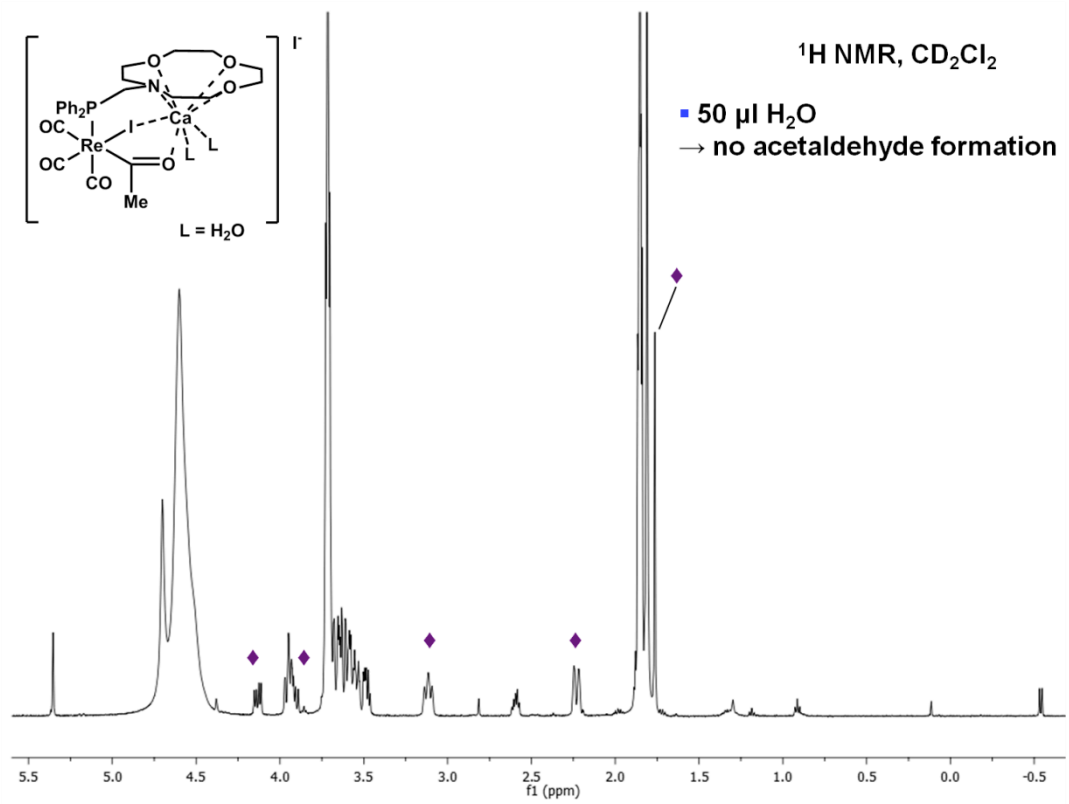

Figure S37. ^{1}H NMR immediately after the addition of 50 µl of H_2O.

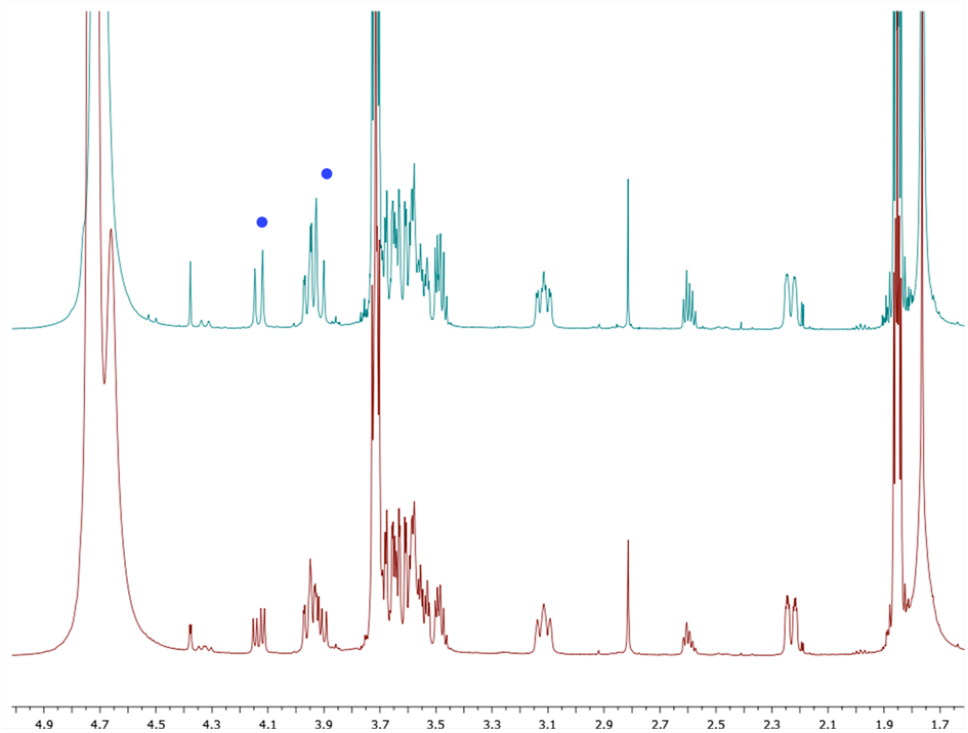

Figure S38. ^{1}H{^{31}P} (top) and ^{1}H (bottom) NMR spectra immediately after the addition of 50 µl of H_2O to **8a**. The PC*H*$_2$ protons are highlighted.

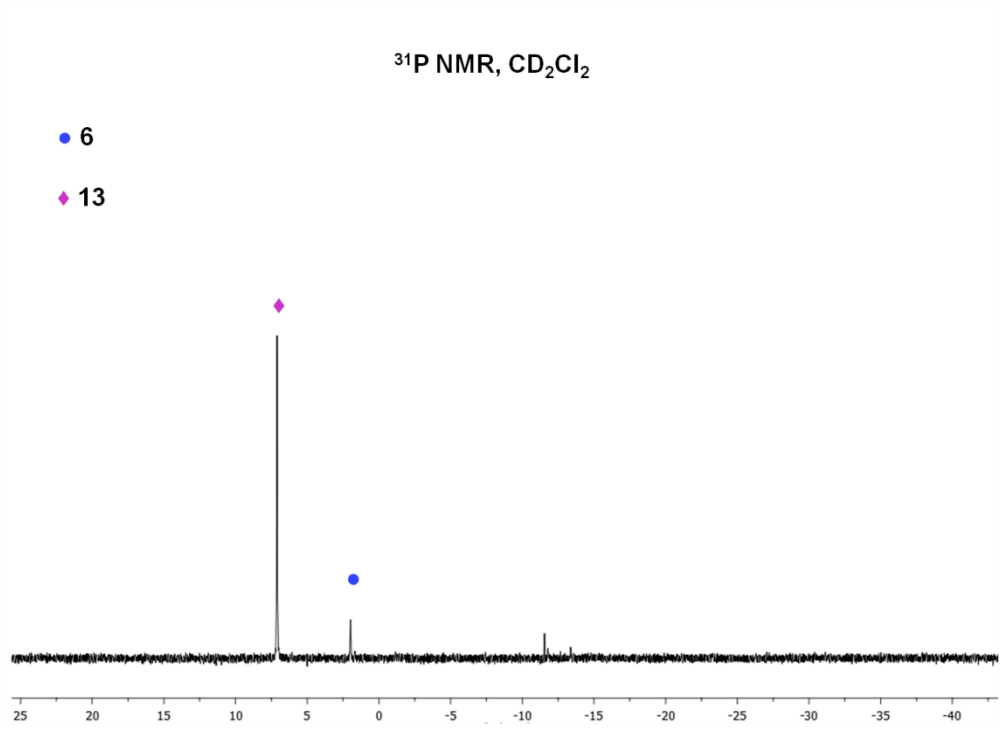

Figure S39. ^{31}P NMR spectrum immediately after the addition of 50 µl of H_2O to **8a**.

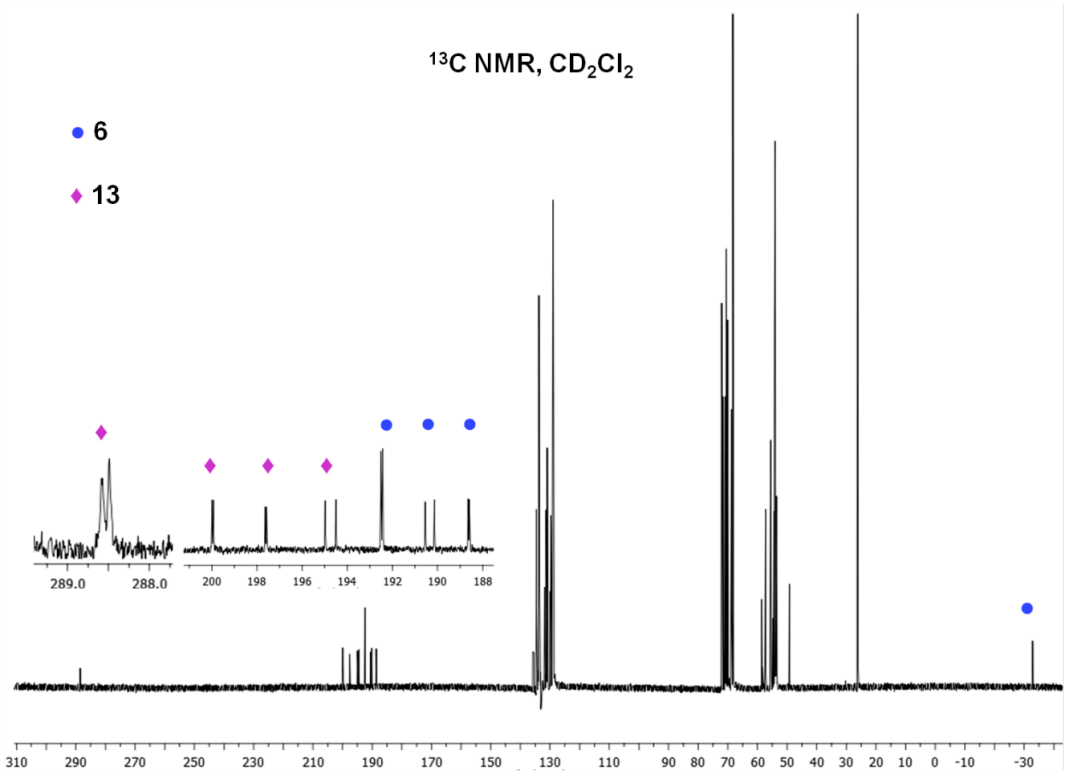

Figure S40. ^{13}C NMR spectrum after the addition of 50 µl of H_2O to **8a**. The spectrum was recorded over a period of 3 h and shows a mixture of **13** and the de-insertion product **6**.

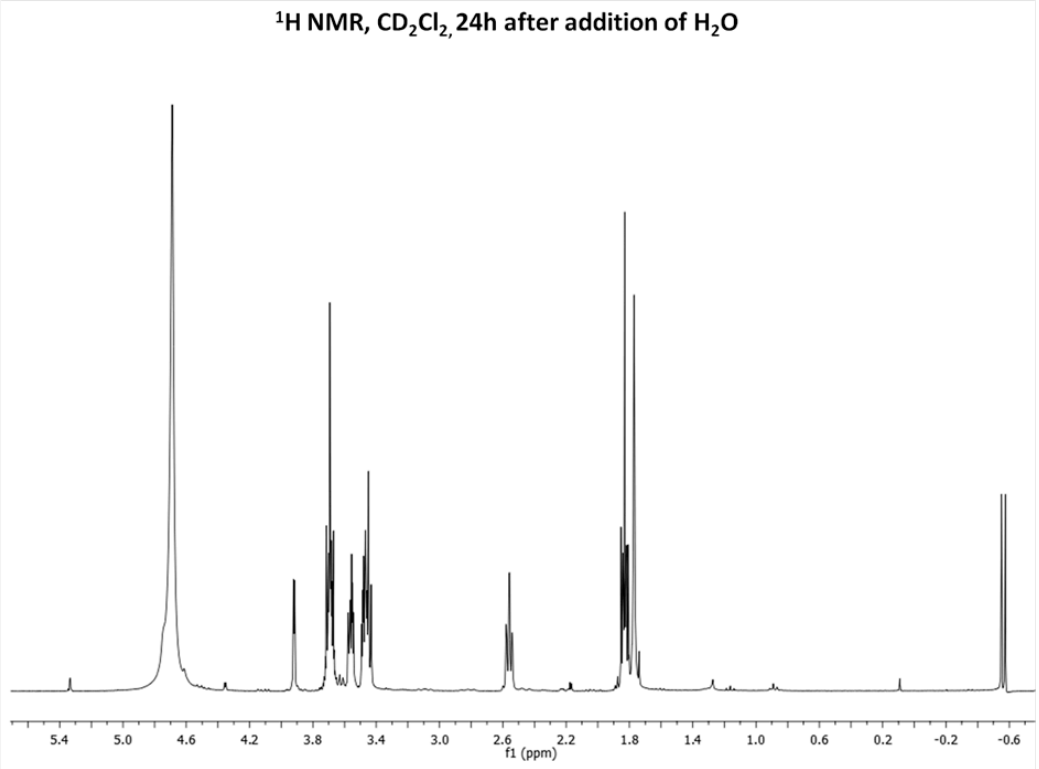

Figure S41. ^{1}H NMR spectrum, 24 h after the addition of 50 µl of H_2O to **8a**, indicating quantitative formation of **6**.

Reaction of 8b with H_2O

Following quantitative formation of the migratory insertion product as assessed by ^{1}H and ^{31}P NMR, 50 µl H_2O (~ 50 equiv) was added to the residue of **8b** suspended in CD_2Cl_2 in a J-Young NMR tube. NMR spectroscopy indicated the formation of acetaldehyde as well as complexes **6** and **12**.

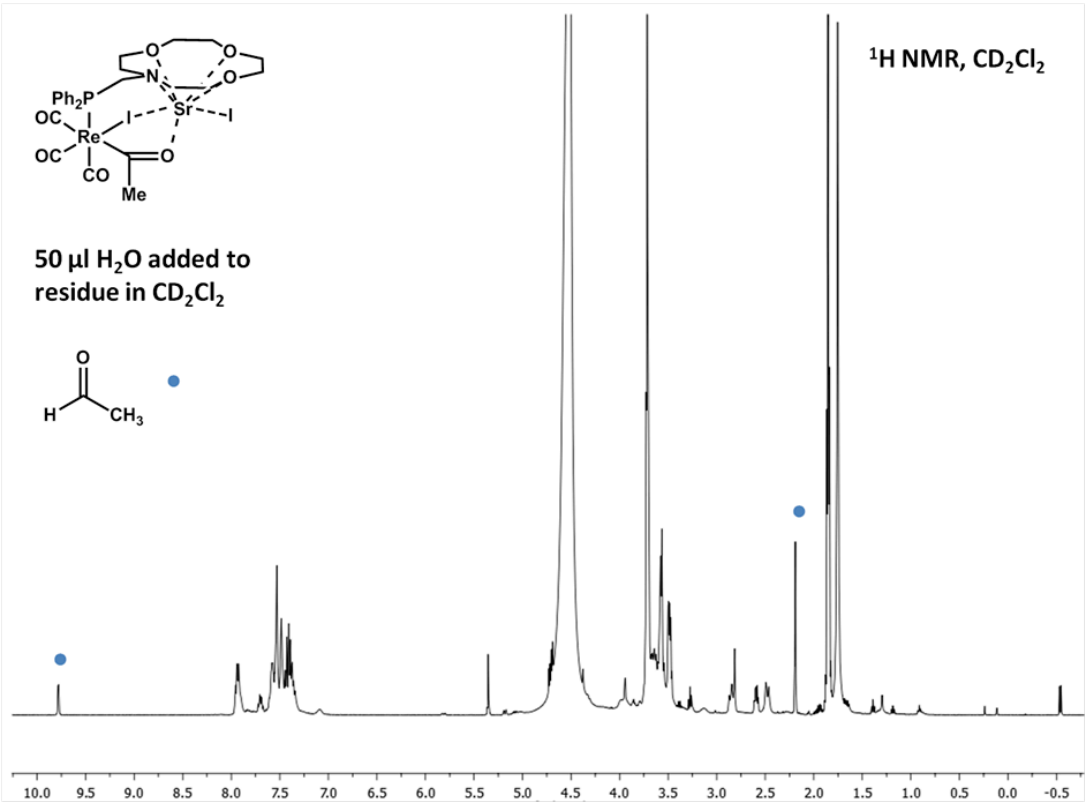

Figure S42.

Reaction of 8a with HOTf

Following quantitative formation of the migratory insertion product **8a**, as assessed by ^{1}H and ^{31}P NMR, 4 µl of HOTf (~ 1 equiv) was added to the J-Young NMR tube containing **8a**. The tube was capped and inverted several times. ^{1}H NMR spectroscopy indicated the immediate formation of acetaldehyde. Additionally, a single metal containing species was observed in the ^{31}P NMR spectrum at – 21 ppm.

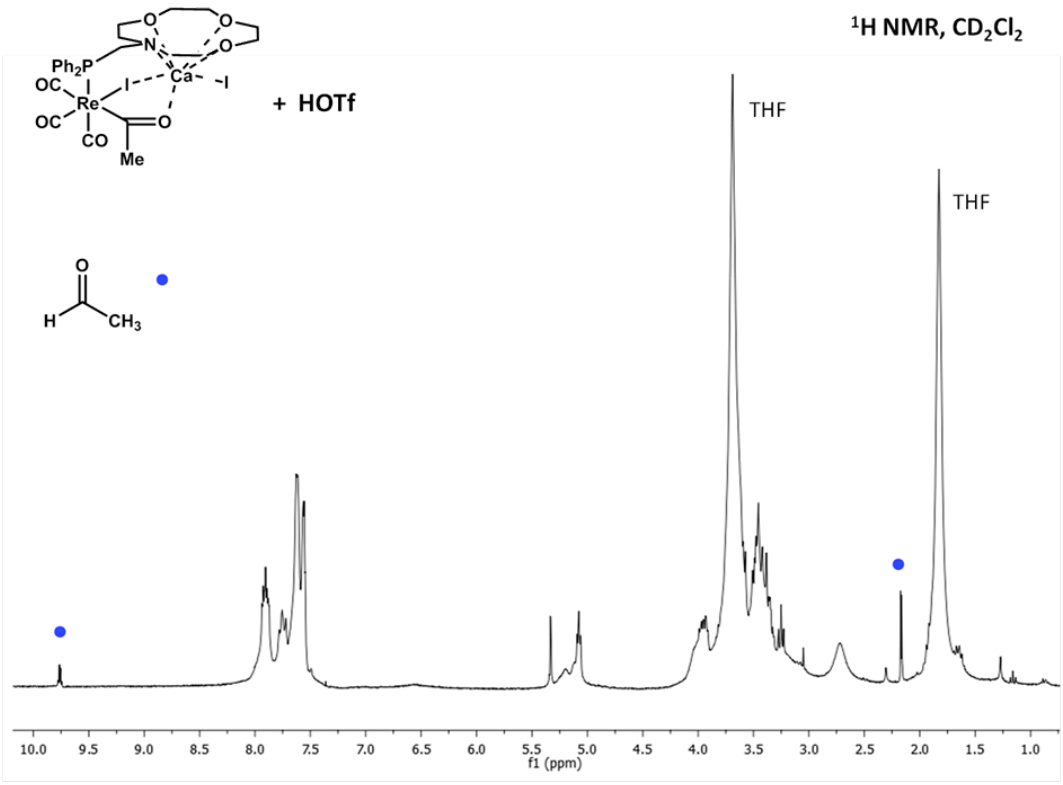

Figure S43. ^{1}H NMR spectrum after the addition of HOTf to **8a**.

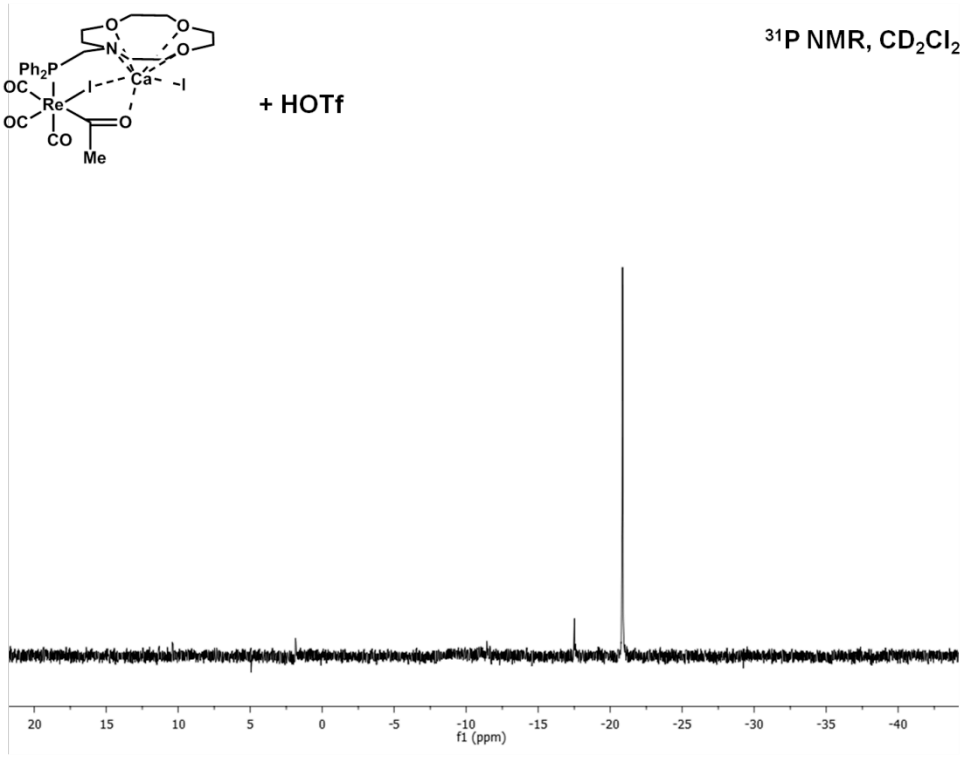

Figure S44. ^{31}P NMR spectrum after the addition of HOTf to **8a**.

Reaction of 8a with HOTf/MeOH

Following quantitative formation of the migratory insertion product **8a**, as assessed by ^{1}H and ^{31}P NMR, 20 µl of MeOH (~ 20 equiv) was added to the J-Young NMR tube containing **8a**. The tube was capped and inverted several times and ^{1}H and ^{31}P NMR spectra were then recorded. No reactivity was observed. Subsequent addition of HOTf (5 µl, ~ 1 equiv) led to the formation of 1,1-dimethoxyethane as well as some methyl iodide, as assessed by ^{1}H NMR spectroscopy.

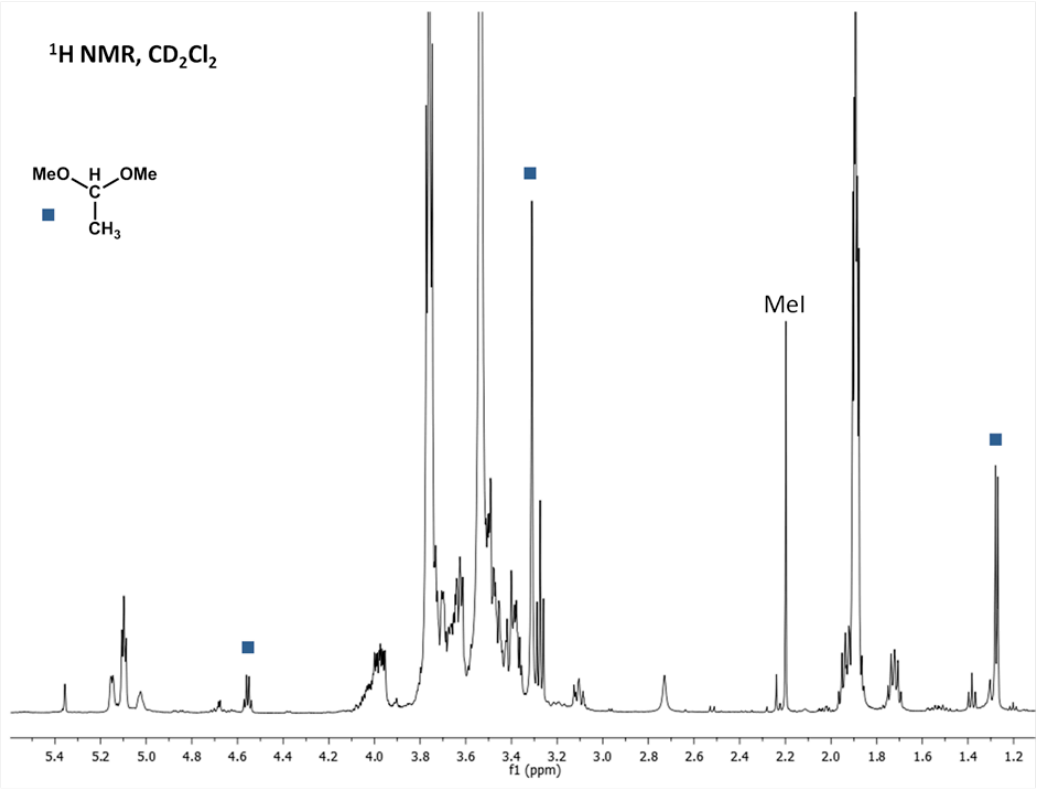

Figure S45. ^{1}H NMR spectrum following the addition of MeOH/HOTf to **8a**.

[Re(CO)$_4$(PNO)I] (12). To a solution of **5** (30 mg, 0.038 mmol) in CH_2Cl_2 (5 ml) was added solid ZnI_2(THF) (16.7 mg, 0.042 mmol). The solution was stirred overnight, passed through a pipette column of alumina to remove the zinc and dried *in vacuo* to afford a white solid. ^{1}H NMR (500 MHz, CD_2Cl_2, δ, ppm): 7.72-7.64 (m, 4H), 7.52-7.46 (m, 6H), 4.35 (d, 2H, J = 2 Hz), 3.58-3.52 (m, 4H), 3.48-3.42 (m, 6H), 2.57 (t, 4H, J = 5 Hz); ^{13}C NMR (125.7 MHz, CD_2Cl_2, δ, ppm): 184.0 (d, 8.8 Hz), 183.2 (d, 6.3 Hz), 182.1 (d, J = 52.8 Hz), 133.9 (d, J = 10.1 Hz), 132.5 (d, J = 44.0 Hz), 131.5 (d, J = 2.6 Hz), 129.1 (d, J = 8.8 Hz), 72.1, 70.5, 70.1, 58.9 (d, J = 26.4 Hz), 55.3 (d, J = 2.5 Hz); ^{31}P NMR (121.5 MHz, CD_2Cl_2, δ, ppm): - 11.5.

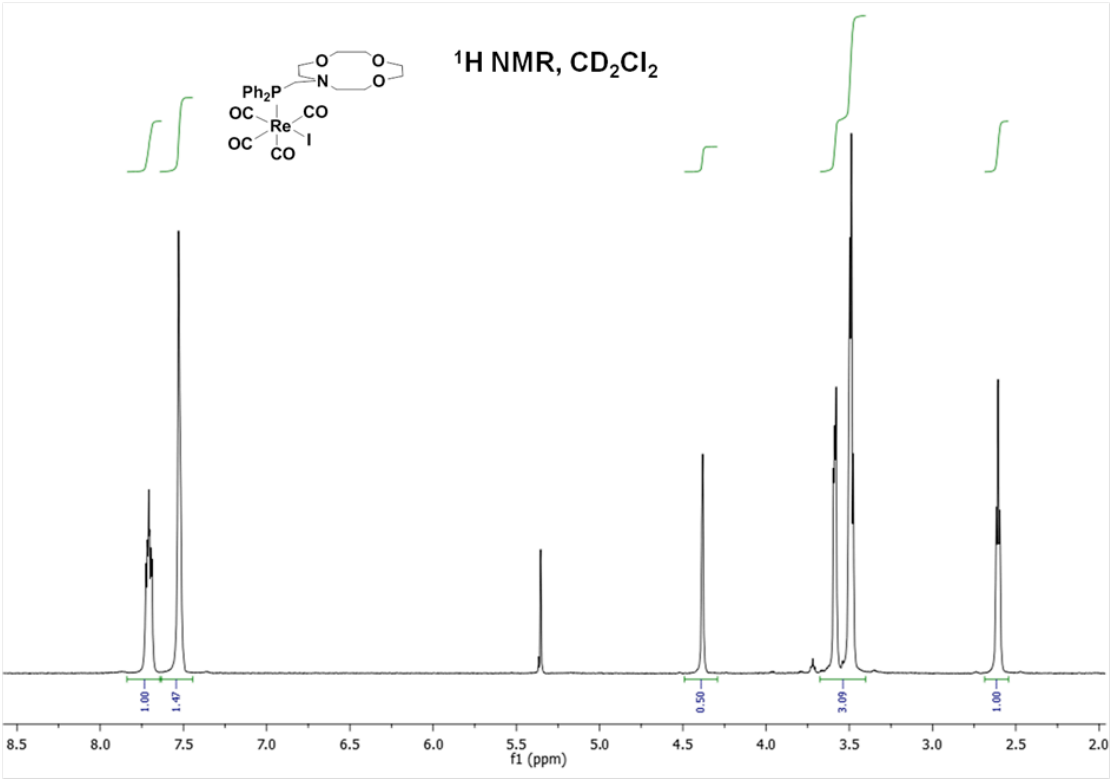

Figure S46. ^{1}H NMR spectrum of **12**.

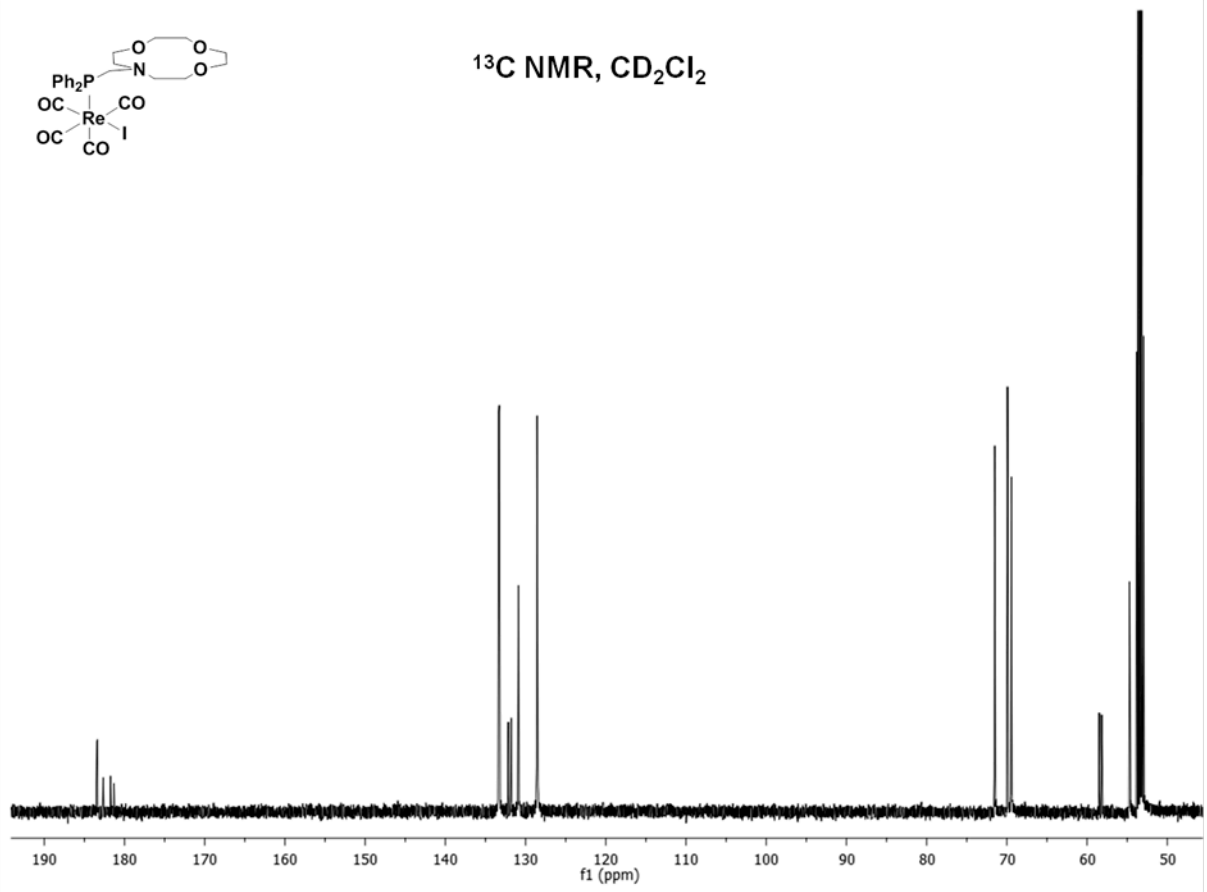

Figure S47. ^{13}C NMR spectrum of **12**.

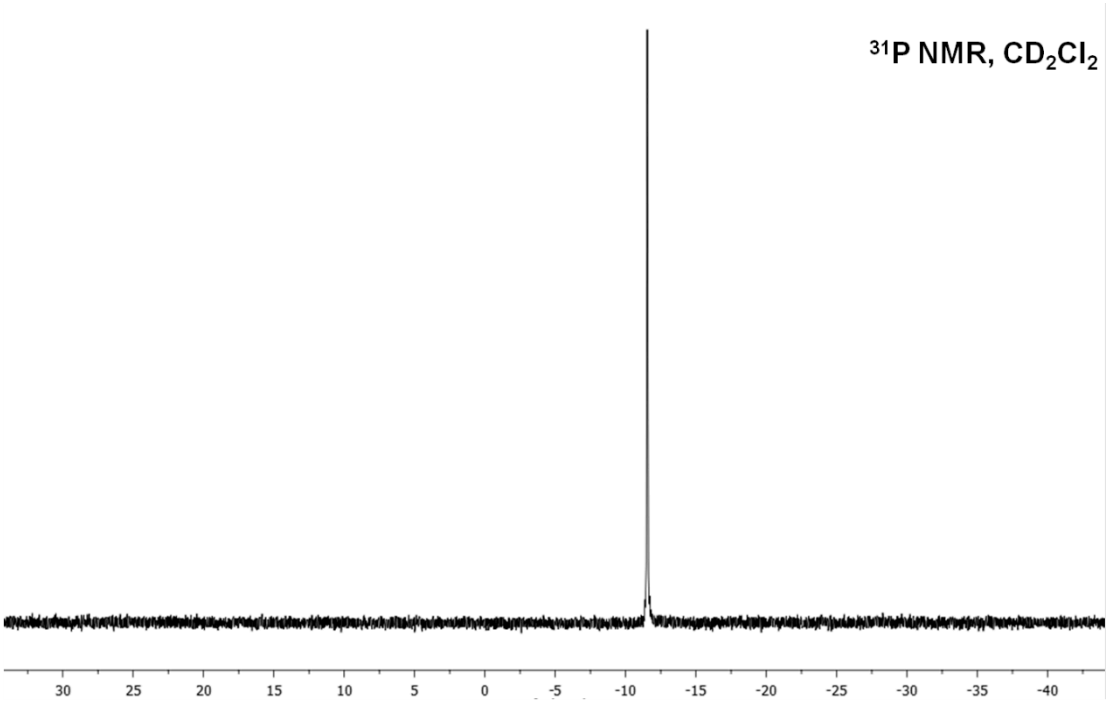

Figure S48. ^{31}P NMR spectrum of **12**.

S5: X-Ray Crystallography Tables

Table 1. Crystal data and structure refinement for AHZ103 (CCDC 850303) (4).

Empirical formula	$[C_{25}H_{28}NO_7PRe]^+ [BF_4]^- \bullet 0.6(C_4H_{10}O)$
Formula weight	801.08
Crystallization Solvent	Dichloromethane/diethyl ether
Crystal Habit	Plate
Crystal size	0.15 x 0.14 x 0.07 mm^3
Crystal color	Colorless

Data Collection

Type of diffractometer	Bruker KAPPA APEX II	
Wavelength	0.71073 Å MoKα	
Data Collection Temperature	100(2) K	
θ range for 9903 reflections used in lattice determination	2.34 to 29.91°	
Unit cell dimensions	a = 9.2994(5) Å b = 9.9376(4) Å c = 17.5007(8) Å	α= 87.062(2)° β= 84.077(3)° γ = 75.087(3)°
Volume	1553.97(13) $Å^3$	
Z	2	
Crystal system	Triclinic	
Space group	P-1	
Density (calculated)	1.712 Mg/m^3	
F(000)	792	
θ range for data collection	2.12 to 33.93°	
Completeness to θ = 33.93°	99.7 %	
Index ranges	$-14 \le h \le 14$, $-15 \le k \le 15$, $-27 \le l \le 27$	
Data collection scan type	ω scans; 22 settings	
Reflections collected	101244	
Independent reflections	12609 [R_{int}= 0.0432]	
Absorption coefficient	4.031 mm^{-1}	
Absorption correction	Semi-empirical from equivalents	
Max. and min. transmission	0.7467 and 0.6282	

Structure solution and Refinement

Structure solution program	SHELXS-97 (Sheldrick, 2008)
Primary solution method	Direct methods
Secondary solution method	Difference Fourier map
Hydrogen placement	Geometric positions
Structure refinement program	SHELXL-97 (Sheldrick, 2008)
Refinement method	Full matrix least-squares on F^2
Data / restraints / parameters	12609 / 28 / 448
Treatment of hydrogen atoms	Riding
Goodness-of-fit on F^2	2.431
Final R indices [I>2σ(I), 11094 reflections]	R1 = 0.0305, *w*R2 = 0.0501
R indices (all data)	R1 = 0.0397, *w*R2 = 0.0508
Type of weighting scheme used	Sigma
Weighting scheme used	$w=1/\sigma^2(Fo^2)$
Max shift/error	0.003
Average shift/error	0.000
Largest diff. peak and hole	2.438 and -2.718 e.Å^{-3}

Special Refinement Details

Crystals were mounted on a glass fiber using Paratone oil then placed on the diffractometer under a nitrogen stream at 100K.

The solvent region of the unit cell is partially occupied by diethyl ether in a somewhat continuous array along the *b*-axis. This was modeled as 0.6 molecules of diethyl ether (isotropic) per asymmetric unit. Additional disorder is observed in the tetrafluoroborate anion which was refined anisotropically in two overlapping orientations..

Refinement of F^2 against ALL reflections. The weighted R-factor (*w*R) and goodness of fit (S) are based on F^2, conventional R-factors (R) are based on F, with F set to zero for negative F^2. The threshold expression of $F^2 > 2\sigma(F^2)$ is used only for calculating R-factors(gt) etc. and is not relevant to the choice of reflections for refinement. R-factors based on F^2 are statistically about twice as large as those based on F, and R-factors based on ALL data will be even larger.

All esds (except the esd in the dihedral angle between two l.s. planes) are estimated using the full covariance matrix. The cell esds are taken into account individually in the estimation of esds in distances, angles and torsion angles; correlations between esds in cell parameters are only used when they are defined by crystal symmetry. An approximate (isotropic) treatment of cell esds is used

for estimating esds involving l.s. planes.

Table 2. Atomic coordinates (x 10^4) and equivalent isotropic displacement parameters ($Å^2$x 10^3) for AHZ103 (CCDC 850303). U(eq) is defined as the trace of the orthogonalized U^{ij} tensor.

	x	y	z	U_{eq}	Occ
Re(1)	8494(1)	-63(1)	6959(1)	19(1)	1
P(1)	6235(1)	-308(1)	7710(1)	19(1)	1
O(1)	8494(2)	-2620(2)	5982(1)	29(1)	1
O(2)	10871(2)	-1989(2)	7883(1)	45(1)	1
O(3)	8608(3)	2196(2)	8121(1)	44(1)	1
O(4)	10800(2)	726(2)	5712(1)	36(1)	1
O(5)	6787(2)	3930(2)	5603(1)	30(1)	1
O(6)	7895(2)	2708(2)	4174(1)	25(1)	1
O(7)	5058(2)	1632(2)	4473(1)	24(1)	1
N(1)	6356(2)	1233(2)	6468(1)	22(1)	1
C(1)	8472(3)	-1678(2)	6325(1)	21(1)	1
C(2)	10012(3)	-1269(3)	7522(1)	28(1)	1
C(3)	8578(3)	1427(3)	7671(1)	29(1)	1
C(4)	9965(3)	442(2)	6176(1)	27(1)	1
C(5)	5245(3)	508(2)	6881(1)	22(1)	1
C(6)	5921(3)	2733(2)	6710(1)	29(1)	1
C(7)	6993(4)	3578(2)	6391(1)	36(1)	1
C(8)	8064(3)	4199(2)	5165(1)	32(1)	1
C(9)	7852(3)	4119(2)	4333(1)	29(1)	1
C(10)	6849(3)	2606(3)	3646(1)	27(1)	1
C(11)	5270(3)	2805(2)	4008(1)	26(1)	1
C(12)	4882(3)	1805(2)	5287(1)	24(1)	1
C(13)	6372(3)	1125(2)	5611(1)	21(1)	1
C(14)	5515(3)	740(2)	8548(1)	22(1)	1
C(15)	4127(3)	1683(2)	8608(1)	25(1)	1
C(16)	3650(3)	2476(3)	9262(1)	29(1)	1
C(17)	4556(3)	2320(3)	9854(1)	34(1)	1
C(18)	5930(3)	1378(3)	9802(2)	41(1)	1
C(19)	6415(3)	581(3)	9155(1)	36(1)	1
C(20)	5889(3)	-1992(2)	7952(1)	20(1)	1
C(21)	4451(3)	-2158(2)	8134(1)	24(1)	1
C(22)	4240(3)	-3465(3)	8340(1)	31(1)	1
C(23)	5464(3)	-4595(3)	8380(1)	30(1)	1
C(24)	6895(3)	-4438(3)	8206(1)	30(1)	1
C(25)	7114(3)	-3142(2)	7986(1)	25(1)	1
B(1B)	8700(8)	5952(8)	2538(4)	64(4)	0.437(4)
F(1B)	9106(5)	6235(8)	1812(3)	63(2)	0.437(4)
F(2B)	9922(3)	5220(5)	2881(2)	50(1)	0.437(4)
F(3B)	7506(3)	5501(5)	2672(2)	45(1)	0.437(4)
F(4B)	8307(6)	7363(6)	2856(4)	65(2)	0.437(4)
B(1C)	8724(7)	6893(8)	2806(5)	46(2)	0.563(4)
F(1C)	7472(4)	6594(5)	3106(4)	136(3)	0.563(4)
F(2C)	8444(3)	8279(3)	2626(2)	45(1)	0.563(4)
F(3C)	9921(3)	6361(5)	3148(3)	77(2)	0.563(4)
F(4C)	8957(8)	6173(6)	2068(4)	152(4)	0.563(4)
C(1C)	210(40)	5739(11)	9875(15)	205(15)	0.293(2)
C(2C)	-364(12)	7272(8)	9554(6)	40(2)	0.293(2)

O(3C)	333(15)	7791(12)	10128(7)	140(5)	0.293(2)
C(4C)	-354(18)	9341(11)	10240(9)	60(5)	0.293(2)
C(5C)	10(13)	10721(8)	9912(6)	27(2)	0.293(2)
C(1D)	853(17)	6125(13)	10238(9)	78(4)	0.293(2)
C(2D)	180(40)	4950(20)	10009(12)	81(5)	0.293(2)
O(3D)	-166(17)	4032(13)	10687(8)	141(5)	0.293(2)
C(4D)	-620(20)	3052(13)	10171(10)	127(7)	0.293(2)
C(5D)	-475(11)	1588(8)	10552(5)	36(2)	0.293(2)

Table 1. Crystal data and structure refinement for AHZ104 (CCDC 822258) (5).

Empirical formula	$[C_{27}H_{31}NO_7PReZn]^+ [BF_4]^- \bullet 0.5(C_6H_6)$
Formula weight	892.96
Crystallization Solvent	Diethyl ether/benzene
Crystal Habit	Plate
Crystal size	0.33 x 0.20 x 0.10 mm^3
Crystal color	Colorless

Data Collection

Type of diffractometer	Bruker KAPPA APEX II	
Wavelength	0.71073 Å MoKα	
Data Collection Temperature	100(2) K	
θ range for 9388 reflections used in lattice determination	2.67 to 38.61°	
Unit cell dimensions	a = 11.5843(6) Å b = 17.2038(8) Å c = 17.2154(9) Å	α= 88.971(3)° β= 77.007(3)° γ = 89.071(3)°
Volume	3342.3(3) $Å^3$	
Z	4	
Crystal system	Triclinic	
Space group	P-1	
Density (calculated)	1.775 Mg/m^3	
F(000)	1764	
θ range for data collection	1.68 to 43.12°	
Completeness to θ = 43.12°	99.0 %	
Index ranges	-22 ≤ h ≤ 22, -30 ≤ k ≤ 33, -33 ≤ l ≤ 33	
Data collection scan type	ω scans; 24 settings	
Reflections collected	338688	
Independent reflections	49331 [R_{int}= 0.0454]	
Absorption coefficient	4.452 mm^{-1}	
Absorption correction	Semi-empirical from equivalents	

Max. and min. transmission	0.6645	and	0.3213

Table 1 (cont.)

Structure solution and Refinement

Structure solution program	SHELXS-97 (Sheldrick, 2008)
Primary solution method	Direct methods
Secondary solution method	Difference Fourier map
Hydrogen placement	Geometric positions
Structure refinement program	SHELXL-97 (Sheldrick, 2008)
Refinement method	Full matrix least-squares on F^2
Data / restraints / parameters	49331 / 0 / 848
Treatment of hydrogen atoms	Riding
Goodness-of-fit on F^2	2.794
Final R indices [I>2σ(I), 37134 reflections]	R1 = 0.0587, *w*R2 = 0.0889
R indices (all data)	R1 = 0.0860, *w*R2 = 0.0907
Type of weighting scheme used	Sigma
Weighting scheme used	$w=1/\sigma^2(Fo^2)$
Max shift/error	0.003
Average shift/error	0.000
Largest diff. peak and hole	8.977 and -4.817 e.Å^{-3}

Special Refinement Details

Crystals were mounted on a glass fiber using Paratone oil then placed on the diffractometer under a nitrogen stream at 100K.

Refinement of F^2 against ALL reflections. The weighted R-factor (*w*R) and goodness of fit (S) are based on F^2, conventional R-factors (R) are based on F, with F set to zero for negative F^2. The threshold expression of $F^2 > 2\sigma(F^2)$ is used only for calculating R-factors(gt) etc. and is not relevant to the choice of reflections for refinement. R-factors based on F^2 are statistically about twice as large as those based on F, and R-factors based on ALL data will be even larger.

All esds (except the esd in the dihedral angle between two l.s. planes) are estimated using the full covariance matrix. The cell esds are taken into account individually in the estimation of esds in distances, angles and torsion angles; correlations between esds in cell parameters are only used when they are defined by crystal symmetry. An approximate (isotropic) treatment of cell esds is used for estimating esds involving l.s. planes.

Table 2. Atomic coordinates (x 10^4) and equivalent isotropic displacement parameters ($Å^2$x 10^3) for AHZ104 (CCDC 822258). U(eq) is defined as the trace of the orthogonalized U^{ij} tensor.

	x	y	z	U_{eq}	Occ
Re(1)	7781(1)	1065(1)	4066(1)	18(1)	1
Zn(1)	6436(1)	2823(1)	1222(1)	16(1)	1
P(1A)	8190(1)	2369(1)	3465(1)	13(1)	1
O(1A)	6960(3)	-534(1)	4816(2)	52(1)	1
O(2A)	8701(2)	368(1)	2379(1)	34(1)	1
O(3A)	10121(2)	997(1)	4674(1)	43(1)	1
O(4A)	6603(3)	1788(2)	5729(2)	28(1)	0.517(4)
O(5A)	5180(3)	1267(2)	3802(3)	30(1)	0.483(4)
O(6A)	7995(2)	2350(1)	424(1)	25(1)	1
O(7A)	6367(2)	3273(1)	-28(1)	27(1)	1
O(8A)	6445(1)	4043(1)	1281(1)	18(1)	1
N(1A)	7842(2)	3006(1)	1906(1)	14(1)	1
C(1A)	7290(3)	53(2)	4541(2)	31(1)	1
C(2A)	8383(2)	615(1)	3000(2)	22(1)	1
C(3A)	9291(2)	1011(1)	4417(1)	24(1)	1
C(4A)	7030(2)	1546(1)	5187(2)	26(1)	0.517(4)
C(4AA)	7030(2)	1546(1)	5187(2)	26(1)	0.483(4)
C(5A)	6049(2)	1204(1)	3844(2)	26(1)	0.483(4)
C(5AA)	6049(2)	1204(1)	3844(2)	26(1)	0.517(4)
C(6A)	9730(2)	2648(1)	3122(1)	15(1)	1
C(7A)	10088(2)	3424(1)	3058(1)	16(1)	1
C(8A)	11250(2)	3615(1)	2709(1)	19(1)	1
C(9A)	12080(2)	3028(1)	2428(1)	19(1)	1
C(10A)	11738(2)	2258(1)	2494(1)	21(1)	1
C(11A)	10576(2)	2063(1)	2839(1)	18(1)	1
C(12A)	7481(2)	3128(1)	4139(1)	16(1)	1
C(13A)	8005(2)	3336(1)	4759(1)	20(1)	1
C(14A)	7412(2)	3831(1)	5354(1)	24(1)	1
C(15A)	6300(2)	4129(1)	5332(2)	26(1)	1
C(16A)	5772(2)	3922(1)	4726(2)	25(1)	1
C(17A)	6347(2)	3417(1)	4133(1)	19(1)	1
C(18A)	7527(2)	2429(1)	2567(1)	14(1)	1
C(19A)	9020(2)	2862(1)	1362(1)	19(1)	1
C(20A)	8959(2)	2209(2)	801(1)	24(1)	1
C(21A)	8285(3)	2625(2)	-371(1)	32(1)	1
C(22A)	7134(3)	2796(2)	-612(2)	34(1)	1
C(23A)	6638(3)	4093(2)	-125(2)	28(1)	1
C(24A)	6067(2)	4454(1)	641(1)	24(1)	1
C(25A)	7448(2)	4351(1)	1508(1)	20(1)	1
C(26A)	7690(2)	3823(1)	2168(1)	18(1)	1
C(27A)	5188(2)	2067(2)	1576(2)	32(1)	1
Re(2)	2950(1)	1026(1)	9107(1)	19(1)	1
Zn(2)	1469(1)	2855(1)	6367(1)	16(1)	1
P(1B)	3400(1)	2332(1)	8512(1)	13(1)	1
O(1B)	2128(2)	-600(1)	9798(2)	51(1)	1
O(2B)	3824(2)	354(1)	7411(1)	39(1)	1
O(3B)	5315(2)	922(1)	9687(1)	38(1)	1
O(4B)	1745(3)	1785(2)	10766(2)	28(1)	0.517(4)
O(5B)	354(4)	1191(2)	8864(3)	32(1)	0.483(4)
O(6B)	3019(2)	2690(1)	5390(1)	29(1)	1

O(7B)	929(2)	3198(1)	5154(1)	26(1)	1
O(8B)	1751(1)	4039(1)	6245(1)	18(1)	1
N(1B)	2990(2)	2952(1)	6968(1)	13(1)	1
C(1B)	2463(3)	-4(2)	9543(2)	32(1)	1
C(2B)	3534(2)	589(1)	8036(2)	23(1)	1
C(3B)	4477(2)	953(1)	9450(1)	24(1)	1
C(4B)	2190(2)	1514(2)	10229(2)	27(1)	0.517(4)
C(4BB)	2190(2)	1514(2)	10229(2)	27(1)	0.483(4)
C(5B)	1219(3)	1172(2)	8910(2)	27(1)	0.483(4)
C(5BB)	1219(3)	1172(2)	8910(2)	27(1)	0.517(4)
C(6B)	4946(2)	2582(1)	8115(1)	15(1)	1
C(7B)	5326(2)	3352(1)	8014(1)	16(1)	1
C(8B)	6473(2)	3530(1)	7620(1)	20(1)	1
C(9B)	7252(2)	2934(1)	7322(1)	19(1)	1
C(10B)	6918(2)	2166(1)	7432(1)	20(1)	1
C(11B)	5763(2)	1987(1)	7825(1)	17(1)	1
C(12B)	2802(2)	3109(1)	9206(1)	19(1)	1
C(13B)	3387(3)	3258(1)	9812(1)	26(1)	1
C(14B)	2853(3)	3760(2)	10432(2)	40(1)	1
C(15B)	1769(3)	4110(2)	10439(2)	42(1)	1
C(16B)	1201(3)	3965(2)	9842(2)	35(1)	1
C(17B)	1707(2)	3463(1)	9228(1)	24(1)	1
C(18B)	2649(2)	2413(1)	7658(1)	14(1)	1
C(19B)	4098(2)	2712(1)	6398(1)	19(1)	1
C(20B)	3820(2)	2231(2)	5739(1)	25(1)	1
C(21B)	2641(3)	2381(2)	4739(2)	37(1)	1
C(22B)	1832(2)	2950(2)	4479(2)	30(1)	1
C(23B)	704(3)	4023(2)	5211(2)	32(1)	1
C(24B)	1629(3)	4420(1)	5509(2)	28(1)	1
C(25B)	2787(2)	4295(1)	6483(1)	19(1)	1
C(26B)	2962(2)	3788(1)	7176(1)	16(1)	1
C(27B)	470(3)	1949(2)	6660(2)	30(1)	1
C(1G)	6520(4)	9772(2)	7928(4)	75(2)	1
C(2G)	6717(4)	9720(3)	7137(4)	84(2)	1
C(3G)	7779(4)	9925(2)	6657(2)	63(1)	1
C(4G)	8653(3)	10179(2)	6996(3)	52(1)	1
C(5G)	8451(4)	10240(2)	7795(3)	70(2)	1
C(6G)	7387(5)	10034(3)	8260(2)	72(2)	1
B(1)	4271(3)	4352(2)	2874(2)	24(1)	1
F(1)	5225(1)	4834(1)	2926(1)	30(1)	1
F(2)	3933(1)	4501(1)	2168(1)	27(1)	1
F(3)	3327(2)	4506(1)	3522(1)	41(1)	1
F(4)	4636(2)	3583(1)	2909(1)	41(1)	1
B(2)	9678(3)	4257(2)	7811(2)	31(1)	1
F(5)	8763(2)	4272(1)	8459(1)	62(1)	1
F(6)	9220(2)	4412(1)	7139(1)	44(1)	1
F(7)	10528(1)	4796(1)	7862(1)	35(1)	1
F(8)	10192(2)	3503(1)	7760(1)	37(1)	1

Table 1. Crystal data and structure refinement for AHZ106 (CCDC 854071).

Empirical formula	$0.8(C_{26}H_{31}NO_7PCaI_2Re)\ 0.2(C_{24}H_{28}NO_6PCaI_3Re)\cdot 2(O)$
Formula weight	1032.54
Crystallization Solvent	Acetonitrile/diethyl ether/water
Crystal Habit	Fragment
Crystal size	0.21 x 0.11 x 0.06 mm^3
Crystal color	Pale yellow

Data Collection

Type of diffractometer	Bruker KAPPA APEX II	
Wavelength	0.71073 Å MoKα	
Data Collection Temperature	100(2) K	
θ range for 9887 reflections used in lattice determination	2.31 to 27.53°	
Unit cell dimensions	a = 11.8734(4) Å b = 14.0152(5) Å c = 12.0094(5) Å	α= 90° β= 109.605(2)° γ = 90°
Volume	1882.61(12) $Å^3$	
Z	2	
Crystal system	Monoclinic	
Space group	P 2_1	
Density (calculated)	1.821 Mg/m^3	
F(000)	979	
θ range for data collection	1.82 to 29.02°	
Completeness to θ = 29.02°	99.8 %	
Index ranges	$-15 \le h \le 16, -19 \le k \le 19, -16 \le l \le 16$	
Data collection scan type	ω scans; 9 settings	
Reflections collected	40053	
Independent reflections	9988 [R_{int}= 0.0455]	
Absorption coefficient	5.251 mm^{-1}	
Absorption correction	Semi-empirical from equivalents	
Max. and min. transmission	0.7587	and 0.3966

Structure solution and Refinement

Structure solution program	SHELXS-97 (Sheldrick, 2008)
Primary solution method	Direct methods
Secondary solution method	Difference Fourier map
Hydrogen placement	Geometric positions
Structure refinement program	SHELXL-97 (Sheldrick, 2008)
Refinement method	Full matrix least-squares on F^2
Data / restraints / parameters	9988 / 1 / 371
Treatment of hydrogen atoms	Riding
Goodness-of-fit on F^2	3.199
Final R indices [I>2σ(I), 9285 reflections]	R1 = 0.0602, *w*R2 = 0.1317
R indices (all data)	R1 = 0.0650, *w*R2 = 0.1322
Type of weighting scheme used	Sigma
Weighting scheme used	$w=1/\sigma^2(Fo^2)$
Max shift/error	0.000
Average shift/error	0.000
Absolute structure parameter	0.109(10)
Largest diff. peak and hole	3.262 and -2.835 e.Å^{-3}

Special Refinement Details

Crystals were mounted on a glass fiber using Paratone oil then placed on the diffractometer under a nitrogen stream at 100K.

This crystal is an inversion twin (refined BASF=0.109) and is disordered at the bridging acetyl position. Twenty per cent of the time this position contains an iodine bridging the Ca and the Re. The disorder was refined without geometric restraints.

Refinement of F^2 against ALL reflections. The weighted R-factor (*w*R) and goodness of fit (S) are based on F^2, conventional R-factors (R) are based on F, with F set to zero for negative F^2. The threshold expression of $F^2 > 2\sigma(F^2)$ is used only for calculating R-factors(gt) etc. and is not relevant to the choice of reflections for refinement. R-factors based on F^2 are statistically about twice as large as those based on F, and R-factors based on ALL data will be even larger.

All esds (except the esd in the dihedral angle between two l.s. planes) are estimated using the full covariance matrix. The cell esds are taken into account individually in the estimation of esds in distances, angles and torsion angles; correlations between esds in cell parameters are only used when they are defined by crystal symmetry. An approximate (isotropic) treatment of cell esds is used

for estimating esds involving l.s. planes.

Table 2. Atomic coordinates (x 10^4) and equivalent isotropic displacement parameters ($Å^2$x 10^3) for AHZ106 (CCDC 854071). U(eq) is defined as the trace of the orthogonalized U^{ij} tensor.

	x	y	z	U_{eq}	Occ
Re(1)	2216(1)	7492(1)	4985(1)	26(1)	1
I(1)	2316(1)	7158(1)	2694(1)	46(1)	1
I(2)	-1591(1)	7403(1)	477(1)	38(1)	1
I(3B)	-73(5)	8344(4)	3988(6)	34(2)	0.205(5)
Ca(4)	442(2)	8827(2)	1572(2)	31(1)	1
P(1)	3301(3)	9001(2)	4994(2)	25(1)	1
O(1)	872(10)	5581(7)	4743(12)	71(3)	1
O(2)	4635(9)	6401(7)	6012(10)	57(3)	1
O(3)	2038(9)	7742(7)	7426(8)	58(3)	1
O(4B)	224(9)	8729(7)	3348(8)	30(2)	0.795(5)
C(4B)	450(20)	8249(14)	4270(20)	33(5)	0.795(5)
C(5B)	-377(14)	8148(11)	4820(15)	38(4)	0.795(5)
O(5)	-208(10)	10458(6)	1597(11)	59(3)	1
O(6)	-604(9)	9504(7)	-409(8)	50(2)	1
O(7)	1724(10)	9089(6)	397(8)	47(2)	1
N(1)	2157(9)	9952(6)	2713(8)	30(2)	1
C(1)	1368(13)	6302(9)	4849(14)	48(3)	1
C(2)	3759(13)	6826(8)	5649(12)	40(3)	1
C(3)	2149(11)	7663(8)	6526(11)	39(3)	1
C(6)	3287(10)	9589(8)	3582(10)	30(2)	1
C(7)	1619(13)	10653(8)	3241(10)	40(3)	1
C(8)	512(12)	11167(9)	2399(11)	40(3)	1
C(9)	-1093(16)	10859(11)	492(16)	62(5)	1
C(10)	-1540(19)	10125(12)	-335(15)	78(6)	1
C(11)	-39(17)	9837(12)	-1059(14)	63(4)	1
C(12)	1080(20)	9177(14)	-926(16)	77(6)	1
C(13)	2672(14)	9681(11)	899(12)	50(4)	1
C(14)	2488(15)	10427(9)	1744(12)	50(4)	1
C(15)	3132(10)	9996(8)	5884(10)	27(2)	1
C(16)	2192(12)	10049(8)	6294(10)	36(3)	1
C(17)	2033(15)	10872(9)	6953(12)	46(4)	1
C(18)	2927(15)	11592(9)	7213(13)	56(4)	1
C(19)	3893(15)	11511(9)	6818(12)	51(4)	1
C(20)	3993(14)	10716(8)	6153(11)	45(3)	1
C(21)	4918(11)	8762(10)	5648(14)	46(4)	1
C(22)	5474(18)	8743(14)	6793(17)	79(6)	1
C(23)	6630(20)	8495(13)	7360(20)	99(8)	1
C(24)	7335(15)	8353(15)	6720(30)	127(12)	1
C(25)	6847(18)	8380(20)	5440(30)	114(9)	1
C(26)	5627(12)	8591(15)	4999(18)	78(6)	1
O(10)	4126(12)	7276(11)	317(13)	109(5)	1
O(11)	5460(20)	8709(18)	1070(20)	181(9)	1

Table 1. Crystal data and structure refinement for AHZ108 (CCDC 854072) (13).

Empirical formula	$[C_{26}H_{31}NO_9PCaIRe]^+[I]^- \bullet 1.5(CH_2Cl_2) \bullet O$
Formula weight	1155.96
Crystallization Solvent	Dichloromethane
Crystal Habit	Plate
Crystal size	0.26 x 0.26 x 0.03 mm^3
Crystal color	Colorless

Data Collection

Type of diffractometer	Bruker KAPPA APEX II	
Wavelength	0.71073 Å MoKα	
Data Collection Temperature	100(2) K	
θ range for 9938 reflections used in lattice determination	2.34 to 27.58°	
Unit cell dimensions	a = 50.446(6) Å b = 8.8199(11) Å c = 17.567(2) Å	α= 90° β= 93.862(7)° γ = 90°
Volume	7798.2(17) $Å^3$	
Z	8	
Crystal system	Monoclinic	
Space group	C 2/*c*	
Density (calculated)	1.969 Mg/m^3	
F(000)	4424	
Data collection program	Bruker APEX2 v2009.7-0	
θ range for data collection	2.32 to 27.97°	
Completeness to θ = 27.97°	99.7 %	
Index ranges	-66 ≤ h ≤ 66, -11 ≤ k ≤ 11, -22 ≤ l ≤ 23	
Data collection scan type	ω scans; 14 settings	
Data reduction program	Bruker SAINT-Plus v7.68A	
Reflections collected	116605	
Independent reflections	9367 [R_{int}= 0.0436]	
Absorption coefficient	5.127 mm^{-1}	
Absorption correction	Semi-empirical from equivalents	
Max. and min. transmission	0.8863 and 0.2887	

Structure solution and Refinement

Structure solution program	SHELXS-97 (Sheldrick, 2008)
Primary solution method	Direct methods
Secondary solution method	Difference Fourier map
Hydrogen placement	Geometric positions
Structure refinement program	SHELXL-97 (Sheldrick, 2008)
Refinement method	Full matrix least-squares on F^2
Data / restraints / parameters	9367 / 6 / 429
Treatment of hydrogen atoms	Riding
Goodness-of-fit on F^2	6.847
Final R indices [I>2σ(I), 8431 reflections]	R1 = 0.0818, *w*R2 = 0.1318
R indices (all data)	R1 = 0.0896, *w*R2 = 0.1320
Type of weighting scheme used	Sigma
Weighting scheme used	$w=1/\sigma^2(Fo^2)$
Max shift/error	0.002
Average shift/error	0.000
Largest diff. peak and hole	4.437 and -3.910 e.Å^{-3}

Special Refinement Details

Crystals were mounted in a loop then placed on the diffractometer under a nitrogen stream at 100K.

The crystal is composed of thin plates slightly rotated from the previous each other. The diffraction clearly shows the presence of multiple crystals (see below) but we were unable integrate the intensities of each separately.

Refinement of F^2 against ALL reflections. The weighted R-factor (*w*R) and goodness of fit (S) are based on F^2, conventional R-factors (R) are based on F, with F set to zero for negative F^2. The threshold expression of $F^2 > 2\sigma(F^2)$ is used only for calculating R-factors(gt) etc. and is not relevant to the choice of reflections for refinement. R-factors based on F^2 are statistically about twice as large as those based on F, and R-factors based on ALL data will be even larger.

All esds (except the esd in the dihedral angle between two l.s. planes) are estimated using the full covariance matrix. The cell esds are taken into account individually in the estimation of esds in distances, angles and torsion angles; correlations between esds in cell parameters are only used when they are defined by crystal symmetry. An approximate (isotropic) treatment of cell esds is used for estimating esds involving l.s. planes.

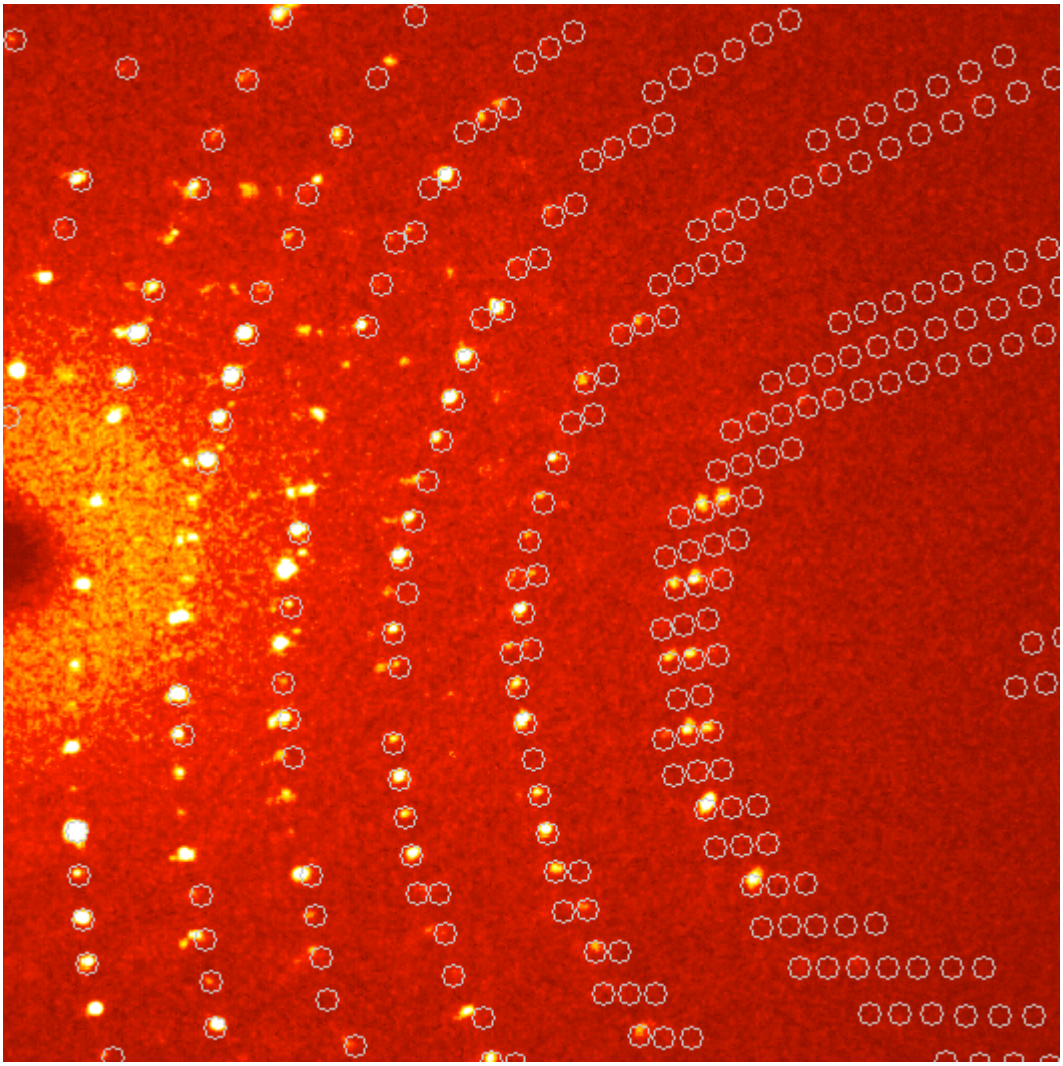

The white circles are the positions of predicted spots.

Table 2. Atomic coordinates (x 10^4) and equivalent isotropic displacement parameters ($Å^2$x 10^3) for AHZ108 (CCDC 854072). U(eq) is defined as the trace of the orthogonalized U^{ij} tensor.

	x	y	z	U_{eq}
Re(1)	8624(1)	2849(1)	-1224(1)	25(1)
I(1)	8990(1)	435(1)	-1002(1)	29(1)
Ca(1)	9281(1)	1866(2)	613(1)	29(1)
P(1)	8401(1)	2053(3)	-86(1)	22(1)
O(1)	8275(2)	722(9)	-2279(4)	45(2)
O(2)	8242(2)	5474(8)	-1518(4)	46(2)
O(3)	8930(2)	3854(8)	-2599(4)	51(2)
O(4)	9014(1)	3749(7)	106(4)	31(2)
O(5)	9589(1)	3982(8)	649(4)	43(2)
O(6)	9633(2)	1008(9)	-117(4)	48(2)
O(7)	9190(1)	2899(7)	1852(4)	30(2)
O(8)	9633(1)	1178(9)	1658(4)	38(2)
O(9)	9282(1)	-820(7)	977(4)	32(2)
N(1)	8792(2)	916(8)	1116(4)	22(2)
C(1)	8821(2)	3486(10)	-2093(7)	35(3)
C(2)	8399(2)	1467(9)	-1877(6)	33(3)
C(3)	8385(2)	4490(12)	-1404(6)	35(3)
C(4)	8914(2)	4343(10)	-439(6)	25(2)
C(5)	8959(2)	5773(12)	-687(6)	41(3)
C(6)	8553(2)	620(9)	601(5)	23(2)
C(7)	8736(2)	2102(10)	1681(5)	23(2)
C(8)	8966(2)	2455(10)	2252(6)	28(2)
C(9)	9426(2)	3104(12)	2344(6)	39(3)
C(10)	9580(2)	1642(14)	2413(7)	46(3)
C(11)	9708(2)	-377(13)	1609(7)	47(3)
C(12)	9470(2)	-1379(13)	1576(6)	45(3)
C(13)	9023(2)	-1506(11)	993(6)	31(2)
C(14)	8858(2)	-577(9)	1484(5)	24(2)
C(15)	8101(2)	954(10)	-370(5)	26(2)
C(16)	7854(2)	1667(11)	-455(6)	34(3)
C(17)	7627(2)	903(13)	-683(6)	39(3)
C(18)	7639(2)	-647(13)	-828(7)	45(3)
C(19)	7886(2)	-1411(12)	-766(6)	38(3)
C(20)	8113(2)	-565(11)	-540(6)	31(2)
C(21)	8276(2)	3529(10)	528(6)	26(2)
C(22)	8119(2)	3120(10)	1129(6)	32(2)
C(23)	8035(2)	4152(11)	1660(6)	34(3)
C(24)	8115(2)	5667(10)	1570(6)	35(3)
C(25)	8264(2)	6107(11)	964(6)	35(3)
C(26)	8346(2)	5026(10)	454(6)	29(2)
C(31)	7700(3)	-92(16)	-2820(8)	68(4)
Cl(1)	7769(1)	702(3)	-3695(2)	63(1)
Cl(2)	7410(1)	-1181(5)	-2914(2)	84(1)
I(2)	9744(1)	7211(1)	-446(1)	50(1)
C(32)	9894(6)	5960(30)	3334(16)	87(12)
Cl(4)	10000	5993(5)	2500	70(2)

Cl(3)	9591(2)	6929(7)	3374(4)	72(2)
O(1S)	8290(3)	2127(11)	2865(7)	115(5)

References

[23] A. B. Pangborn, M. A. Giardello, R. H. Grubbs, R. K. Rosen, F. J. Timmers, *Organometallics* **1996**, *15*, 1518.
[24] E. W. H. Abel, G. B.; Wilkinson, G. J., *J. Chem. Soc* **1958**, 3149.
[25] K. M. Fromm, *CrystEngComm* **2002**, *4*, 318.
[26] F. Ramirez, R. Sarma, Y. F. Chaw, T. M. McCaffrey, J. F. Marecek, B. McKeever, D. Nierman, *J. Am. Chem. Soc.* **1977**, *99*, 5285.
[27] L. E. Manzer, *Inorg. Synth.* **1982**, *21*, 135.